UCL Université catholique de Louvain

École polytechnique de Louvain (EPL)

# Value of storage in smart grids

Dissertation presented by
**Arnaud FABRI**

for obtaining the Master's degree in
**Mathematical Engineering**

Supervisor(s)
**Anthony PAPAVASILIOU, Gauthier DE MAERE D'AERTRYCKE**

Reader(s)
**Yves SMEERS**

Academic year 2016-2017

**Acknowledgments**

I would like to express my gratitude to my two supervisors, Anthony Papavasiliou and Gauthier de Maere d'Aertrycke, for their support and their guidance during this whole semester.

A particular thanks to Anthony, for introducing me to the energy world and electricity markets last year, in such an interesting way that I decided to make my master thesis out of it. Thanks also for the friendly conversations we had this year, whether it was directly concerning my thesis or not.

I would also like to thank Gauthier for the welcome at ENGIE's office and the help he could provide me for the models and the codes that are used in this thesis.

I thank Yves Smeers for agreeing to be part of my jury and taking the time to read my thesis.

Besides, I would also like to thank Niels Leemput and Yuting Mou, who both gave me useful data for this thesis.

My final thanks goes to everyone I shared this five amazing years at university with, especially my fellow students, my roommates, my friends and my family.

**Disclaimer** : "The views set out in this study are those of the author and do not necessarily reflect the opinion of ENGIE."

# Contents

**Introduction** **1**

**1 Optimal power flow formulation** **3**
1.1 Branch flow model . . . 3
1.2 SOCP Relaxation of the branch flow model . . . 5
1.3 Exactness of the convex relaxation . . . 7
1.3.1 Angle recovery condition . . . 7
1.3.2 Angle recovery algorithm for radial networks . . . 8
1.3.3 Exactness of the SOCP-BFM solution . . . 8
1.4 Dual formulation of the SOCP relaxation . . . 9
1.5 Conclusion of chapter 1 . . . 12

**2 Multi-time-step OPF problem with energy storage capacity expansion** **13**
2.1 SOCP formulation of the problem . . . 13
2.2 Dual formulation of the multi-time step OPF problem . . . 16
2.3 Conclusion of Chapter 2 . . . 19

**3 A case study on a realistic European distribution network** **20**
3.1 Materials and data . . . 20
3.1.1 Distribution grid . . . 20
3.1.2 Residential load and solar generation profiles . . . 21
3.2 Modeling assumptions and network constraints . . . 21
3.2.1 Active power . . . 21
3.2.2 Reactive Power . . . 22
3.2.3 Voltage control . . . 22
3.2.4 Battery Storage Modeling . . . 22
3.2.5 Objective function . . . 24
3.3 Conclusion of Chapter 3 . . . 25

**4 Results and analysis** **26**
4.1 Behavior without storage . . . 26
4.1.1 Without voltage constraint (case 1A and 1B) . . . 26
4.1.2 Realistic case with voltage constraints (case 2A and 2B) . . . 28
4.2 Battery energy storage investment . . . 36
4.2.1 Base case (3A and 3B) . . . 36
4.2.2 Impact of prices on optimal investment in batteries . . . 39
4.3 "Off-grid" distribution network (e.g. island) . . . 39
4.3.1 Comparison between centralized storage and decentralized storage . . . 41
4.4 Running time of the algorithm . . . 42
4.5 Conclusion of Chapter 4 . . . 43

**5 Optimal investment from a prosumer point of view** **44**
5.1 Uniform pricing . . . . . 44
5.2 Day-Night Pricing . . . . . 45
5.3 Prosumer pricing . . . . . 46
5.4 Bidirectional Pricing . . . . . 48
5.5 Conclusion of Chapter 5 . . . . . 49

**Extensions** **50**

**Conclusion** **52**

# Notations

| | |
|---|---|
| $\|z\|$ | Magnitude of the complex number $z$. |
| $\angle z$ | Argument of the complex number $z$. |
| $z^*$ | Complex conjugate of the complex number $z$. |
| $Re\{z\}$ | Real part of the complex number z. |
| $\|x\|_2$ | 2-norm of vector $x$, $\|x\|_2 := \sqrt{x_1^2 + ... + x_n^2}$. |
| $\mathcal{L}^n$ | Second order cone (Lorentz cone), $\mathbb{L}^n := \{(x_0, x_1, ..., x^n) \in \mathbb{R}^{n+1} \mid \quad x_0 \geq \|(x_1, ..., x_n)\|_2\}$. |
| | |
| $\mathcal{N}$ | Set of nodes composing the network, $\mathcal{N} := \{0, 1, .., n\}$. |
| $\mathcal{N}_+$ | Set of nodes except the substation node, $\mathcal{N}_+ := \{1, .., n\}$. |
| $\mathcal{E}$ | Set of lines composing the network, $\mathcal{E} := \{1, .., n\}$. |
| $A_i$ | Unique ancestor node of node $i$. |
| $C_i$ | Set of children nodes of node $i$. |
| $z_i$ | Complex impedance of line $i$, $z_i := r_i + \mathbf{i}x_i$. |
| $r_i$ | Resistance of line $i$. |
| $x_i$ | Reactance of line $i$. |
| $V_i$ | Complex voltage at node $i$. |
| $I_i$ | Complex current on line $i$. |
| $s_i$ | Power injection (production minus consumption) at node $i$, $s_i := p_i + \mathbf{i}q_i$. |
| $p_i$ | Real power injection (production minus consumption) at node $i$, $p_i := p_i^g - p_i^c$. |
| $q_i$ | Reactive power injection (production minus consumption) at node $i$, $q_i := q_i^g - q_i^c$. |
| $p_i^g$ | Real power generation at node $i$. |
| $p_i^c$ | Real power consumption at node $i$. |
| $q_i^g$ | Reactive power generation at node $i$. |
| $q_i^c$ | Reactive power consumption at node $i$. |
| $S_i$ | Sending-end complex power of line $i$, $S_i := P_i + \mathbf{i}Q_i$. |
| $P_i$ | Real power flow on line $i$. |
| $Q_i$ | Reactive power flow on line $i$. |
| $v_i$ | Magnitude squared of voltage at node $i$, $v_i := \|V_i\|^2$. |
| $l_i$ | Magnitude squared of current on line $i$, $l_i : \|I_i\|^2$. |
| $C_i^g$ | Marginal cost of generating power at node $i$. |
| $C_i^c$ | Marginal benefit of consuming power at node $i$. |
| $e_i, t$ | Energy stored at node $i$ and time $t$. |
| $f_i$ | Maximal storage capacity at node $i$. |
| $p_{i,t}^{in}$ | Active power input in the battery at node $i$ and time $t$. |
| $p_{i,t}^{out}$ | Active power output from the battery at node $i$ and time $t$. |
| $\eta$ | Round-trip efficiency of the battery. |
| $\xi^{in}$ | Charging efficiency factor of the battery. |
| $\xi^{out}$ | Discharging efficiency factor of the battery. |

# List of Figures


1.1 Representation of line $i$ . . . 3

3.1 Schematic representation of the residential distribution network used . . . 21

4.1 Average voltage behavior on the line (case 1A) . . . 27
4.2 Voltage behavior across the line for critical hours (case 1A) . . . 27
4.3 Total curtailment due to line limits, in both cases a total of ± 33kWh of solar are curtailed out of 4035kWh potential solar production (<1%). . . . 28
4.4 Average voltage behavior on the line (case 2A) . . . 29
4.5 Voltage behavior along the line for critical hours (case 2A). . . . 29
4.6 Voltage profiles through a day of high solar production for an average consumer (case 2B) . . . 30
4.7 Voltage profiles through a day of high demand an no solar production, for an average consumer (case 2A) . . . 30
4.8 Curtailment behavior and local prices at peak solar hour, case 3A. . . . 32
4.9 Total curtailment over 4 weeks per households compared to the capacity of production. . . . 33
4.10 Average local prices on the line (case 2B) . . . 34
4.11 Total curtailment over 4 weeks per households compared to the capacity of production 35
4.12 Optimal battery investment (Inv cost = 300€/kWh) . . . 36
4.13 Case 3B, but we fix 4 kWh of storage at node 29 bis. . . . 38
4.14 Energy level in the battery during one winter day compared to solar production of the whole network. Case 3B, but we fix 4 kWh storage at node 29 bis. . . . 38
4.15 Evolution of local marginal prices at node 29bis during one winter day. . . . 39
4.16 Evolution of optimal storage investment as a function of investment cost. Case 3A, case 3B is similar. . . . 40
4.17 Total curtailment per household over 4 weeks compared to the capacity of production, "island" case. . . . 41
4.18 Optimal battery investment in "island" case (Inv cost = 300€/kWh). . . . 41
4.19 Total curtailment over 4 weeks per household compared to the capacity of production, "island" case with storage. . . . 42

5.1 Total curtailment over 4 weeks compared to the capacity of production in the case of "Prosumer Pricing". . . . 47

# Introduction

The distribution systems (DSOs networks) are taking a more and more important place in global power system operations. Traditionally, they had (and still have) a very passive role: retail and commercial consumers use as much power as they need and are charged a predefined price for it, generally fixed per unit of energy consumed or in a time-of-use pricing scheme. However, we currently see the emergence of low-voltage networks with a high-share of solar photovoltaics panels and a lot more demand flexibility, which will be increasing with the integration of electric vehicles in the network. These new distribution network configurations with decentralized generation, demand flexibility and possibly energy storage are often called "smart grids".

The distribution grids are usually not much coordinated with the rest of the system and the decentralized production is absent from the wholesale electricity market. Therefore, the co-optimization of distribution networks (DSO) and transmission networks (TSO) is a very important topic of research at the moment, see [1], [2] for example. In this work, we will focus on system operations at a distribution network level. More specifically, we wish to assess the potential of storage in a low-voltage grid with high levels of decentralized generation.

The optimal power flow problem (OPF) is looking for the optimal way of dispatching power through a network as a function of the network characteristics, physical electrical constraints such as Kirchoff's laws, the supply of generators and the load of the consumers. It can be extended to include various problematics such as unit commitment, reserve scheduling, demand response... This problem is difficult to solve even in its easiest formulation due to non-linearities and non-convexity of power flow equations. In the last decades, the common practice has been to use a direct current (DC) approximation of the OPF problem for transmission networks. This DC-OPF approximation is a linearization of the original alternative current formulation (AC-OPF). However, this approximation is not well-suited for distribution grid operations since it ignores power flow components such as reactive power and voltage constraints that play an important role in low-voltage grid configurations.

The challenge is to solve instances of AC-OPF that are computationally tractable and that take network constraints into account. Therefore, in the recent years a lot of work has been done to obtain convex relaxations or linearizations of the AC-OPF problem [3], [4][5], [6], [7], [8] [9]. In this work, we will use a SOCP relaxation of the ACP-OPF and extend it to integrate storage capacity expansion. Other optimal storage investment studies for low-voltage network such as [10] usually use a linearized version of AC-OPF.

The recent interest for batteries in low-voltages grid is triggered by different factors. First, high decentralized generation in distribution systems that were not designed for it are pushing the network to its limits. The distribution network operator has to make sure that constraints such as line limits or voltage quality are respected and that may lead to a curtailment of decentralized production, i.e. not allowing the so-called prosumers (producers-consumers) to re-inject as much power in the network as they wish. This phenomenon can be an incentive for capacity expansion of the network both on the side of the distribution network operator and on the prosumer side

(install batteries to store energy in case of curtailment). Secondly, the price of batteries are currently being driven down by the lot of research that is done in the field and the increased demand coming from applications such as electric vehicles.

The goals of this work are multiple. First, we want to have a better understanding of network behavior in case of high decentralized generation by identifying voltage, curtailment and locational marginal prices profiles. Secondly, we wish to evaluate the impact of storage integration on those profiles as well as the economical profitability of investing in storage. Finally, this is the occasion to illustrate the computational tractability of the SOCP formulation of AC-OPF in capacity expansion problems, for investment horizons that take seasonal effect into account.

This thesis will be organized as follow:

- The first chapter will present how to derive the SOCP relaxation from the non-convex power flow equations. A condition for exactness of this relaxation is presented as well as a dualization of the problem.
- In the second chapter, we extend the problem formulation of chapter 1 in a multi-time-step formulation that take storage possibilities into account. It also contains the dual formulation together with a brief dual analysis.
- The third chapter presents materials and data we used to make our simulations. It also presents realistic assumptions on network constraints and battery characteristics modeling.
- The fourth chapter is the key chapter of this thesis as it contains the most important results we obtained on our test network. We present socially optimal operations of the system for different cases. The social optimum is defined by minimizing the total cost of running the whole system. We go from a simple power flow problem without voltage constraints, to a realistic operation of the network with voltage constraints, to finish with a study of the optimal sizing and placement of storage in the network. Particular attention is paid to the effect of the position of the prosumer with regard to the location of substation node.
- The fifth chapter presents principal models of pricing power to the prosumer. The goal is to evaluate the effects of the pricing models in a high-decentralized generation framework. We also wish to identify if they provide incentives for the prosumer to behave in the socially optimal way presented in chapter 4.
- We conclude by proposing other capacity expansion problems that could be interesting and a review of the main results we obtained.

# Chapter 1

# Optimal power flow formulation

Convex relaxations of the OPF for distribution networks using his radial properties have been widely studied in the last decade [3] [5], [6], [9],[11]. The two main models that have been studied are the bus injection model and the branch flow model. A summary of the two models, their relaxations and the equivalences between them is presented in [7] and [8].

In this work, we will use a formulation of the branch flow model as described in [5],[6]. Indeed, this model was claimed to have good scaling properties.

## 1.1 Branch flow model

We model a distribution network as a connected directed tree graph $\mathcal{G} := (\mathcal{N}, \mathcal{E})$. The set of nodes $\mathcal{N} := \{0, 1, ..., n\}$ represents the set of buses of the network and the set $\mathcal{E}$ represents the distribution lines connecting them. We index the root node, i.e. the substation that connects the distribution network to the transmission network, by 0. Any other node $i \in \mathcal{N}_+ := \mathcal{N} \setminus \{0\}$ has a unique ancestor $A_i$. Every node has also a set of children $C_i$. We arbitrarily choose the orientation of the graph where every line points towards the the root, so that every line is oriented from $i$ to $A_i$. This allow us, we can index every line by the index of its origin node $i$ and the set of lines is $\mathcal{E} := \{1, ..., n\}$.

We will now define both nodal and branch variables on this network, which is the specificity of the branch flow model compared to bus injection model (only nodal variables). A schematic representation of one line is represented at figure 1.1.

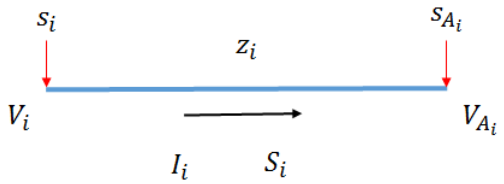


Figure 1.1: Representation of line $i$

For each node $i \in \mathcal{N}$, we define

- $V_i$ as the complex voltage
- $s_i = p_i + q_i$ as the complex net power injection (the net power injection being power production minus power consumption).

For each line $i \in \mathcal{E}$, we define

- $z_i = r_i + \mathbf{i}x_i$ as the complex impedance of the line
- $I_i$ as the complex current
- $S_i = P_i + \mathbf{i}Q_i$ the sending-end complex power, where $P_i$ denote the active power and $Q_i$ the reactive power.

The branch flow model is then defined by the following equations :

$$V_i - V_{A_i} = z_i I_i \qquad \forall i \in \mathcal{E} \tag{1.1.1}$$
$$S_i = V_i I_i^* \qquad \forall i \in \mathcal{E} \tag{1.1.2}$$
$$S_i = s_i + \sum_{j \in C_i} (S_j - z_j |I_j|^2) \qquad \forall i \in \mathcal{N} \tag{1.1.3}$$

where equation (1.1.1) represents Ohm's Law, (1.1.2) the branch power definition and (1.1.3) the power balance at each node. For the power balance equation at substation node, we define $S_0 = 0$ for ease and consider the injection from transmission network is represented by $s_0$. Note that we do not consider shunt admittance to the ground in this work. To incorporate them, we should add a term in equation (1.1.3).

We will then add some more constraints to get an optimal power flow problem over a distribution network. We can first impose bounds on net power injections at each node:

$$\underline{s_i} \leq s_i \leq \overline{s_i} \qquad \forall i \in \mathcal{N}. \tag{1.1.4}$$

Note that equation (1.1.4) can be used to define power generation limit and power consumption at each node. Indeed, if we let $s_i = s_i^g - s_i^c$, instead of (1.1.4) we can impose

$$\underline{s_i^g} \leq s_i^g \leq \overline{s_i^g} \quad \forall i \in \mathcal{N}, \tag{1.1.5}$$

for power generation and

$$\underline{s_i^c} \leq s_i^c \leq \overline{s_i^c} \quad \forall i \in \mathcal{N}, \tag{1.1.6}$$

for power consumption.

Another constraint for distribution networks is that voltage magnitudes should be maintained in acceptable range :

$$\underline{v_i} \leq |V_i|^2 \leq \overline{v_i} \qquad \forall i \in \mathcal{N}. \tag{1.1.7}$$

Finally, we express line limits in terms of branch flow currents:

$$0 \leq |I_j|^2 \leq \overline{I_i} \qquad \forall i \in \mathcal{E}. \tag{1.1.8}$$

If we express our problem simply in terms of the variables $x := (S, s, V, I)$, we can define an objective function $C(x)$ and our optimal power flow problem can be written as

$$\text{OPF-BFM1 :} \qquad \min_x \quad C(x)$$
$$s.t. \quad (1.1.1) - (1.1.4), (1.1.7) - (1.1.8).$$

## 1.2 SOCP Relaxation of the branch flow model

A SOCP relaxation of OPF-BFM1 can be obtained in two steps [5], [11]. First we will express our model in terms of real variables and therefore eliminate voltage and current angles. Then, we will relax a quadratic equality constraint into a quadratic inequality to obtain a conic program.

Let us define $l_j = I_j I_j^*, \forall j \in \mathcal{E}$ and $v_j = V_i V_i^*, \forall i \in \mathcal{N}$.

Taking magnitudes squared, Ohm's law constraint (1.1.1) can be transformed in

$$\begin{aligned}
V_i - V_{A_i} &= z_i I_i && \forall i \in \mathcal{E} \\
V_{A_i} &= V_i - z_i I_i && \forall i \in \mathcal{E} \\
V_{A_i} V_{A_i}^* &= (V_i - z_i I_i)(V_i - z_i I_i)^* && \forall i \in \mathcal{E} \\
v_{A_i} &= v_i - V_i I_i^* z_i^* - z_i I_i V_i^* + z_i I_i I_i^* z_i^* && \forall i \in \mathcal{E} \\
v_{A_i} &= v_i - S_i z_i^* - z_i S_i^* + z_i l_i z_i^* && \forall i \in \mathcal{E} \\
v_{A_i} &= v_i - 2\mathrm{Re}\{S_i z_i^*\} + z_i l_i z_i^* && \forall i \in \mathcal{E}.
\end{aligned}$$

By recalling that $z_i = r_i + \mathbf{i}x_i$ and $S_i = P_i + \mathbf{i}Q_i$, we can express Ohm's Law in terms of real variables,

$$v_{A_i} = v_i - 2(r_i P_i + x_i Q_i) + (r_i^2 + x_i^2) l_i \qquad \forall i \in \mathcal{E}. \tag{1.2.1}$$

Similarly, we can transform constraint (1.1.2) in

$$\begin{aligned}
S_i &= V_i I_i^* && \forall i \in \mathcal{N}_+ \\
S_i S_i^* &= V_i I_i^* I_i V_i^* && \forall i \in \mathcal{E} \\
|S_i|^2 &= v_i l_i && \forall i \in \mathcal{E} \\
P_i^2 + Q_i^2 &= v_i l_i && \forall i \in \mathcal{E}.
\end{aligned} \tag{1.2.2}$$

Constraints (1.1.3) can be easily decomposed in terms of real variables as follow

$$P_i = p_i + \sum_{j \in C_i} (P_j - r_j l_j) \qquad \forall i \in \mathcal{N}_+ \tag{1.2.3}$$

$$Q_i = q_i + \sum_{j \in C_i} (Q_j - x_j l_j) \qquad \forall i \in \mathcal{N}_+ \tag{1.2.4}$$

$$0 = p_0 + \sum_{j \in C_0} (P_j - r_j l_j) \tag{1.2.5}$$

$$0 = q_0 + \sum_{j \in C_0} (Q_j - x_j l_j), \tag{1.2.6}$$

because we imposed $S_0 = P_0 + \mathbf{i}Q_0 = 0$ for ease. Similarly, for constraint (1.1.4) we have

$$\underline{p_i} \leq p_i \leq \overline{p_i} \qquad \forall i \in \mathcal{N} \tag{1.2.7}$$

$$\underline{q_i} \leq q_i \leq \overline{q_i} \qquad \forall i \in \mathcal{N}. \tag{1.2.8}$$

Again equations (1.2.7) and (1.2.8) can be used to constraint power generation limits and power consumption at each node by letting $p_i = p_i^g - p_i^c$, $q_i = q_i^g - q_i^c$ and instead of (1.2.7), (1.2.8), imposing

$$\underline{p_i^g} \leq p_i^g \leq \overline{p_i^g} \qquad \forall i \in \mathcal{N} \tag{1.2.9}$$
$$\underline{q_i^g} \leq q_i^g \leq \overline{q_i^g} \qquad \forall i \in \mathcal{N}, \tag{1.2.10}$$

for power generation and

$$\underline{p_i^c} \leq p_i^c \leq \overline{p_i^c} \qquad \forall i \in \mathcal{N} \tag{1.2.11}$$
$$\underline{q_i^c} \leq q_i^c \leq \overline{q_i^c} \qquad \forall i \in \mathcal{N}. \tag{1.2.12}$$

for power consumption.

Equations (1.1.7) and (1.1.8) simply become

$$\underline{v_i} \leq v_i \leq \overline{v_i} \qquad \forall i \in \mathcal{N}. \tag{1.2.13}$$

$$0 \leq l_i \leq \overline{l_i} \qquad \forall i \in \mathcal{E}. \tag{1.2.14}$$

We can now express our problem in terms of the real variables $x := (P, Q, p, q, v, l) \in \mathbb{R}^{6n+3}$ or even $x := (P, Q, p^g, p^c, q^g, q^c, v, l) \in \mathbb{R}^{8n+5}$ and we obtain a branch flow model where we have removed the phase-angles (denoted below as "angle relaxed branch flow model"):

$$\text{AR-BFM}: \quad \min_x \quad C(x) \qquad s.t. \quad (1.2.1) - (1.2.6), (1.2.9) - (1.2.14). \tag{1.2.15}$$

The feasible set of AR-BFM is still non-convex due to the quadratic equalities in (1.2.2). To obtain a convex model, we relax them into the inequalities

$$P_i^2 + Q_i^2 \leq v_i l_i \quad \forall i \in \mathcal{E}, \tag{1.2.16}$$

which is a rotated second-order cone constraint, hence convex. The reformulation of the rotated second-order cone in a second-order cone constraint can be done as follow:

$$\begin{aligned}
P_i^2 + Q_i^2 &\leq v_i l_i \\
4P_i^2 + 4Q_i^2 &\leq 4 v_i l_i \\
4P_i^2 + 4Q_i^2 &\leq (v_i + l_i)^2 - (v_i - l_i)^2 \\
(2P_i)^2 + (2Q_i)^2 + (v_i - l_i)^2 &\leq (v_i + l_i)^2 \\
\|2P_i \quad 2Q_i \quad (v_i - l_i)\|_2 &\leq (v_i + l_i) \\
\begin{pmatrix} v_i + l_i \\ v_i - l_i \\ 2P_i \\ 2Q_i \end{pmatrix} &\in \mathbb{L}^3,
\end{aligned}$$

where $\mathbb{L}^3$ is a Lorentz cone. The Lorentz cone $\mathbb{L}^n$ is defined as

$$\mathbb{L}^n := \{(x_0, x_1, ..., x^n) \in \mathbb{R}^{n+1} | \quad x_0 \geq \|(x_1, ..., x_n)\|_2\}.$$

We finally arrive to our second order cone relaxation of our relaxation by considering (1.2.16) instead of (1.2.2)

$$\begin{aligned} \text{SOCP-BFM}: \quad & \min_{x} \quad C(x) \\ & s.t. \quad (1.2.1), (1.2.3)-(1.2.6), (1.2.9)-(1.2.14), (1.2.16). \end{aligned} \tag{1.2.17}$$

If we choose to minimize a convex objective function C(x) the above conic problem is convex. For instance, we can aim to minimize line losses on the network

$$C(x) = \sum_{i \in \mathcal{E}} r_i l_i, \tag{1.2.18}$$

or minimize real power generation costs and maximize consumers benefits

$$C(x) = \sum_{i \in \mathcal{N}} C_i^g p_i^g - \sum_{i \in \mathcal{N}} C_i^c p_i^c, \tag{1.2.19}$$

where $C_i^p$ is the marginal cost of generator $i$, $C_i^c$ is the marginal benefit of consumer $i$.

## 1.3 Exactness of the convex relaxation

We have made two successive relaxations of OPF-BFM to obtain the SOCP-BFM. It is clear that when OPF-BFM is feasible, SOCP-BFM will also be feasible and will provide a lower bound to the original problem. How and when is this relaxation is exact ? This question can be divided in two parts :

1. From a solution of AR-BFM, can we recover the phase angles and therefore a solution of the original OPF-BFM problem ?
2. Does the solution of the SOCP-BFM satisfy the equality (1.2.2) and is therefore also an exact solution of AR-BFM ?

### 1.3.1 Angle recovery condition

The angle recovery condition is stated in theorem 2 of [5] as follow :

The angle recovery condition holds if and only if for every cycles $c$ in $G$

$$\sum_{(i,A_i) \in c} \beta_i = 0 \mod 2\pi, \tag{1.3.1}$$

where $\beta_i := \angle(v_i - z_i^* S_i), \quad \forall i \in \mathcal{E}$. Informally, $\beta_i$ represents the phase angle difference across edge $i$ due to the angle relaxation.

Since we make the hypothesis our distribution network is radial, there is no cycle and the angle recovery condition is trivially satisfied. Based on an optimal solution of AR-BFM, we can therefore always recover an optimal solution of OPF-BFM with the angle recovery algorithm of section 1.3.2.

### 1.3.2 Angle recovery algorithm for radial networks

An angle recovery algorithm is presented in [5], for meshed networks where condition (1.3.1) is satisfied. We will only present here a simpler version for radial networks.

We wish to recover the variables $x := (S, s, V, I)$ from the solution expressed in terms of variables $x := (P, Q, p, q, v, l)$.

1. First, recall that $S_i = P_i + \mathbf{i}Q_i$, $s_i = p_i + \mathbf{i}q_i$, $v_i = V_i V_i^* = |V_i|^2$ and $l_i = I_j I_j^* = |I_i|^2$. We can recover $|V_i| = \sqrt{v_i}$ and $|I_i| = \sqrt{l_i}$. Hence, we only need to recover phases angles for current and voltage, i.e. $\angle V_i$ and $\angle I_i$.
2. Fix the voltage angle at substation node, $\angle V_0 = 0$.
3. Then go down the distribution network following
   - $\angle I_i = \angle V_{A_i} - \angle(S_i - r_i l_i - \mathbf{i}x_i l_i)$
   - $\angle V_i = \angle S_i + \angle I_i$ .

### 1.3.3 Exactness of the SOCP-BFM solution

The exactness of the relaxation can always be checked a posteriori by checking if the inequality (1.2.16) is tight. There are also some conditions that can be checked a priori and that guarantees the exactness of the relaxation [8]. We will here use the sufficient condition that is presented in theorem 1 of [5].

**Proposition 1.** *If we allow infinite power consumption at each node, i.e.* $\overline{p_i^c} = \overline{q_i^c} = \infty, \forall i \in \mathcal{N}$, *relaxing equality* (1.2.2) *in inequality* (1.2.16) *is an exact relaxation, therefore any optimal solution of SOCP-BFM is also optimal for AR-BFM.*

**Remark 1.** *The theorem of proposition 1 and its proof in [5] are based on some assumptions :*

1. *The network graph $G$ is connected.*
2. *The cost function $C(x)$ is convex.*
3. *The cost function $C(x)$ is strictly increasing in $l$, non-increasing in load $s^c$ and independent of $S$.*
4. *The original optimal power flow problem is feasible.*

*These assumptions seem reasonable, assumption 2) and 3) are for example satisfied for an objective function as described in* (1.2.18). *Would $C(x)$ only be non-decreasing in $l$ instead of strictly increasing in $l$ (e.g.* (1.2.19)*, we can only assure that there is* ***one*** *optimal solution of SOCP-BFM that is also optimal for AR-BFM. Indeed, there may be other optimal solutions of SOCP-BFM with strict inequality $P_i^2 + Q_i^2 < v_i l_i$, that are therefore non-feasible for AR-BFM. To tackle this problem, we can check a posteriori if our optimal solution of SOCP satisfies $P_i^2 + Q_i^2 = v_i l_i$. If it is not the case we can for example add a term that is strictly increasing in $l$ in our objective, $\tilde{C}(x) = C(x) + \epsilon \sum_{i \in \mathcal{E}} l_i, \epsilon > 0$.*

**Remark 2.** *Recall that the conditions of the theorem are sufficient but not necessary conditions, as shown in [8]. There are many instances of SOCP-BFM where the relaxation is exact even though $\overline{p_i^c}, \overline{q_i^c} < \infty$.*

## 1.4 Dual formulation of the SOCP relaxation

In order to perform a sensitivity analysis of the model it can be useful to derive the dual formulation of the problem. For conic optimization the standard primal-dual pair is as follows:

$$\begin{aligned} &\max_y b^T y && \min_x c^T x \\ &A^T y \preceq_K c && Ax = b \\ & && x \succeq_{K^*} 0 \end{aligned} \tag{1.4.1}$$

where the relation $A^T y \preceq_K c$ is equivalent to $c - A^T y \succeq_K 0 \Leftrightarrow c - A^T y \in K$. $K^*$ is the dual of cone $K$, in our case we have only conic constraints of $\mathbb{R}^n_+$ (linear inequalities) and $\mathbb{L}^m$ (second order cone constraints), our cone $K = \mathbb{R}^n_+ \times \mathbb{L}^m$ will be a self-dual cone (because $\mathbb{R}^n_+$ and $\mathbb{L}^m$ are self-dual), hence we have $K = K^*$.

To dualize, let us rewrite our model SOCP-BFM (1.2.17) in almost (equality constraints can be transformed into two inequality constraints) standard form as follows:

$$(Primal): \quad \max \quad \sum_{i\in\mathcal{N}} C_i^c p_i^c - \sum_{i\in\mathcal{N}} C_i^g p_i^g \tag{1.4.2}$$

$$(\beta_i): \quad v_{A_i} = v_i - 2(r_i P_i + x_i Q_i) + (r_i^2 + x_i^2) l_i, \quad \forall i \in \mathcal{E} \tag{1.4.3}$$

$$(\lambda_0): \quad 0 = p_0^g - p_0^c + \sum_{j\in C_0} (P_j - r_j l_j) \tag{1.4.4}$$

$$(\lambda_i): \quad P_i = p_i^g - p_i^c + \sum_{j\in C_i} (P_j - r_j l_j), \quad \forall i \in \mathcal{N}_+ \tag{1.4.5}$$

$$(\mu_0): \quad 0 = q_0^g - q_0^c + \sum_{j\in C_0} (Q_j - x_j l_j) \tag{1.4.6}$$

$$(\mu_i): \quad Q_i = q_i^g - q_i^c + \sum_{j\in C_i} (Q_j - x_j l_j), \quad \forall i \in \mathcal{N}_+ \tag{1.4.7}$$

$$(\delta_i^{g+}): \quad p_i^g \le \overline{p_i^g}, \quad \forall i \in \mathcal{N} \tag{1.4.8}$$

$$(\delta_i^{g-}): \quad \underline{p_i^g} \le p_i^g, \quad \forall i \in \mathcal{N} \tag{1.4.9}$$

$$(\delta_i^{c+}): \quad p_i^c \le \overline{p_i^c}, \quad \forall i \in \mathcal{N} \tag{1.4.10}$$

$$(\delta_i^{c-}): \quad \underline{p_i^c} \le p_i^c, \quad \forall i \in \mathcal{N} \tag{1.4.11}$$

$$(\theta_i^{g+}): \quad q_i^g \le \overline{q_i^g}, \quad \forall i \in \mathcal{N} \tag{1.4.12}$$

$$(\theta_i^{g-}): \quad \underline{q_i^g} \le q_i^g, \quad \forall i \in \mathcal{N} \tag{1.4.13}$$

$$(\theta_i^{c+}): \quad q_i^c \le \overline{q_i^c}, \quad \forall i \in \mathcal{N} \tag{1.4.14}$$

$$(\theta_i^{c-}): \quad \underline{q_i^c} \le q_i^c, \quad \forall i \in \mathcal{N} \tag{1.4.15}$$

$$(\sigma_i^+): \quad v_i \le \overline{v_i}, \quad \forall i \in \mathcal{N} \tag{1.4.16}$$

$$(\sigma_i^-): \quad \underline{v_i} \le v_i, \quad \forall i \in \mathcal{N} \tag{1.4.17}$$

$$(\eta_i^+): \quad l_i \le \overline{l_i}, \quad \forall i \in \mathcal{E} \tag{1.4.18}$$

$$(\eta_i^-): \quad 0 \le l_i, \quad \forall i \in \mathcal{E} \tag{1.4.19}$$

$$\begin{pmatrix} \gamma_{1i} \\ \gamma_{2i} \\ \gamma_{3i} \\ \gamma_{4i} \end{pmatrix}: \quad \begin{pmatrix} v_i + l_i \\ v_i - l_i \\ 2P_i \\ 2Q_i \end{pmatrix} \in \mathbb{L}^3, \quad \forall i \in \mathcal{E}. \tag{1.4.20}$$

The names for dual multipliers are inspired by the names chosen in [12]. Note that we have formulated our primal problem as a maximization problem to ease the duality, although in practice we will rather use a minimization formulation

$$\min C(x) = \min \sum_{i\in\mathcal{N}} C_i^g p_i^g - \sum_{i\in\mathcal{N}} C_i^c p_i^c, \tag{1.4.21}$$

in numerical simulations. This has no influence on the optimal solution, it just changes the sign of the objective value.

Applying dual relationship (1.4.1), we obtain the following dual problem:

$$\begin{aligned}
(Dual): \quad \min \quad & \sum_{i\in\mathcal{N}} (\overline{p_i^g}\delta_i^{g+} - \underline{p_i^g}\delta_i^{g-} + \overline{p_i^c}\delta_i^{c+} - \underline{p_i^c}\delta_i^{c-} \\
& + \overline{q_i^g}\theta_i^{g+} - \underline{q_i^g}\theta_i^{g-} + \overline{q_i^c}\theta_i^{c+} - \underline{q_i^c}\theta_i^{c-}) \\
& + \sum_{i\in\mathcal{N}} (\overline{v_i}\sigma_i^+ - \underline{v_i}\sigma_i^-) \\
& + \sum_{i\in\mathcal{E}} \overline{l_i}\eta_i^+
\end{aligned} \tag{1.4.22}$$

$$(P_i): \quad -2r_i\beta_i + \lambda_i - \lambda_{A_i} - 2\gamma_{3i} = 0, \quad \forall i \in \mathcal{E} \tag{1.4.23}$$

$$(Q_i): \quad -2x_i\beta_i + \mu_i - \mu_{A_i} - 2\gamma_{4i} = 0, \quad \forall i \in \mathcal{E} \tag{1.4.24}$$

$$(p_i^g): \quad -\lambda_i + (\delta_i^{g+} - \delta_i^{g-}) + C_i^g = 0, \quad \forall i \in \mathcal{N} \tag{1.4.25}$$

$$(p_i^c): \quad \lambda_i + (\delta_i^{c+} - \delta_i^{c-}) - C_i^c = 0, \quad \forall i \in \mathcal{N} \tag{1.4.26}$$

$$(q_i^g): \quad -\mu_i + (\theta_i^{g+} - \theta_i^{g-}) = 0, \quad \forall i \in \mathcal{N} \tag{1.4.27}$$

$$(q_i^c): \quad \mu_i + (\theta_i^{c+} - \theta_i^{c-}) = 0, \quad \forall i \in \mathcal{N} \tag{1.4.28}$$

$$(v_i): \quad \beta_i - \sum_{j\in C_i} \beta_j + (\sigma_i^+ - \sigma_i^-) - \gamma_{1i} - \gamma_{2i} = 0, \quad \forall i \in \mathcal{N}_+ \tag{1.4.29}$$

$$(v_0): \quad -\sum_{j\in C_0} \beta_j + (\sigma_0^+ - \sigma_0^-) = 0 \tag{1.4.30}$$

$$(l_i): \quad (r_i^2 + x_i^2)\beta_i + r_i\lambda_{A_i} + x_i\mu_{A_i} + (\eta_i^+ - \eta_i^-) - \gamma_{1i} + \gamma_{2i} = 0, \quad \forall i \in \mathcal{E} \tag{1.4.31}$$

$$\delta_i^{g+}, \delta_i^{g-}, \delta_i^{c+}, \delta_i^{c-}, \theta_i^{g+}, \theta_i^{g-}, \theta_i^{c+}, \theta_i^{c-}, \sigma_i^+, \sigma_i^- \geq 0, \quad \forall i \in \mathcal{N} \tag{1.4.32}$$

$$\eta_i^+, \eta_i^- \geq 0, \quad \forall i \in \mathcal{E} \tag{1.4.33}$$

$$\begin{pmatrix} \gamma_{1i} \\ \gamma_{2i} \\ \gamma_{3i} \\ \gamma_{4i} \end{pmatrix} \in \mathbb{L}^3, \quad \forall i \in \mathcal{E}. \tag{1.4.34}$$

Some the dual multipliers have an economical or physical interpretation. Dual variables of the power balance equations, i.e. $\lambda_i$ and $\mu_i$, represent the local marginal prices of respectively active and reactive power at each node. In literature, $\lambda_i$ is sometimes called "locational" marginal prices to make the distinction with "local" prices in the transmission network. In this thesis, we are only dealing with distribution networks and therefore "locational" prices although we sometimes refer to them as "local" prices for ease. $\sigma_i^+, \sigma_i^-$ can be interpreted as the marginal value of relaxing (or constraining) the voltage at each node and $\eta_i^+, \eta_i^-$ as the marginal value of additional line capacity.

Looking at constraints of the dual now, from (1.4.25), we can see that $(\delta_i^{g+} - \delta_i^{g-})$ is equal to the difference between price and the marginal production cost for generator $i$, i.e. the scarcity

rent for generator $i$. Looking at constraints (1.4.26)-(1.4.28), we can hold a similar reasoning for $(\delta_i^{c+} - \delta_i^{c-}), (\theta_i^{g+} - \theta_i^{g-}), (\theta_i^{c+} - \theta_i^{c-})$. Note that constraints (1.4.23), (1.4.24) allow us to isolate $\gamma_{3i}, \gamma_{4i}$ and by combining (1.4.29), (1.4.31) we can also isolate $\gamma_{1i}, \gamma_{2i}$. Re-injecting in (1.4.34) would give us a non-linear relation between $\lambda_i, \lambda_{A_i}, \mu_i, \mu_{A_i}, (\sigma_i^+ - \sigma_i^-), (\eta_i^+ - \eta_i^-), \beta_i, \sum_{j \in C_i} \beta_j$ . This illustrates the non-linear links between prices $\lambda_i, \mu_i$ at node $i$ and the prices at ancestor node $\lambda_{A_i}, \mu_{A_i}$. This also shows that there seems to be no relation for real power price as as a function of real power price at ancestor/children nodes alone, real power and reactive power prices being linked in a non-linear way. A more elaborated decomposition of locational marginal prices based on the KKT optimality conditions of the SOCP-BFM, is developed in [12].

One of the issues we wish to analyze in this thesis is decentralized solar production curtailment. Therefore, let us have a look at some of the KKT conditions concerning real power generation/consumption:

$$0 \leq \delta_i^{g+} \perp \overline{p_i^g} - p_i^g \geq 0, \qquad \forall i \in \mathcal{N} \tag{1.4.35}$$
$$0 \leq \delta_i^{g-} \perp p_i^g - \underline{p_i^g} \geq 0, \qquad \forall i \in \mathcal{N} \tag{1.4.36}$$
$$0 \leq \delta_i^{c+} \perp \overline{p_i^c} - p_i^c \geq 0, \qquad \forall i \in \mathcal{N} \tag{1.4.37}$$
$$0 \leq \delta_i^{c-} \perp p_i^c - \underline{p_i^c} \geq 0, \qquad \forall i \in \mathcal{N} \tag{1.4.38}$$
$$-\lambda_i + (\delta_i^{g+} - \delta_i^{g-}) + C_i^g = 0, \qquad \forall i \in \mathcal{N} \tag{1.4.39}$$
$$\lambda_i + (\delta_i^{c+} - \delta_i^{c-}) - C_i^c = 0, \qquad \forall i \in \mathcal{N} \tag{1.4.40}$$

**Proposition 2.** *From the KKT above we have :*

1. *If a prosumer (producer/consumer) is producing at peak capacity ($p_i^g = \overline{p_i^g}$) then the local marginal price is greater than his marginal production cost, $\lambda_i \geq C_i^g$. If he is consuming is maximum load ($p_i^c = \overline{p_i^c}$) then $\lambda_i \leq C_i^c$.*
2. *If a prosumer is producing at minimum capacity ($p_i^g = \underline{p_i^g}$) then the local marginal price is less than his marginal production cost, $\lambda_i \leq C_i^g$. If he is consuming minimal load ($p_i^c = \underline{p_i^c}$) then $\lambda_i \geq C_i^c$.*
3. *If a prosumer is producing strictly within his production range ($\underline{p_i^g} < p_i^g < \overline{p_i^g}$) then the local marginal price is equal to his marginal production cost, $\lambda_i = C_i^g$. If he is consuming strictly in his consumption range ($\underline{p_i^c} < p_i^c < \overline{p_i^c}$) then $\lambda_i = C_i^c$.*

*Proof.* The results are simply derived from the KKT conditions. For example, if we consider a prosumer producing strictly within his production range ($\underline{p_i^g} < p_i^g < \overline{p_i^g}$) from (1.4.35) and (1.4.36), we have $\delta_i^{g+} = \delta_i^{g-} = 0$. Then, equation (1.4.39) simplifies in $\lambda_i = C_i^g$. Proofs of other assumptions are similar. □

This proposition highlights the direct link between the socially optimal behavior of a prosumer at a particular node and the local marginal price at this same node. For example, in case of solar generation curtailment, the producer is not producing at his full capacity ($\underline{p_i^g} < p_i^g < \overline{p_i^g}$), and therefore we have $\lambda_i = C_i^g$. In case of solar production, if we assume there is no marginal cost of producing ($C_i^g = 0$), solar curtailment phenomenon is characterized by a zero local marginal price at this node. In this line of thinking, the nodal marginal prices $\lambda_i$ could be seen as incentive for each prosumers to behave in a socially optimal way.

Indeed, suppose each prosumer is facing a real time marginal local node pricing $\lambda_i$ for buying and selling real power, then the maximization of his own benefits can be put as the following optimization problem:

$$\max_{p_i^g, p_i^c} \quad (\lambda_i - C_i^g)p_i^c - (C_i^C - \lambda_i)p_i^c \tag{1.4.41}$$

$$(\delta_i^{g+}): \quad p_i^g \leq \overline{p_i^g} \tag{1.4.42}$$

$$(\delta_i^{g-}): \quad \underline{p_i^g} \leq p_i^g \tag{1.4.43}$$

$$(\delta_i^{c+}): \quad p_i^c \leq \overline{p_i^c} \tag{1.4.44}$$

$$(\delta_i^{c-}): \quad \underline{p_i^c} \leq p_i^c \tag{1.4.45}$$

$$\tag{1.4.46}$$

The KKT optimality conditions for this problem are exactly (1.4.35)-(1.4.40), meaning that the socially optimal solution computed by the full problem (1.4.2) would also be considered optimal by each of his participants. However, any solution of the problem of (1.4.41) is not necessary optimal for the full problem. Consider for example the case $\lambda_i = C_i^g$, from an individual perspective, any choice of $\underline{p_i^g} \leq p_i^g \leq \overline{p_i^g}$ is optimal for prosumer $i$ (it does not affect is own benefit), therefore his choice might not correspond to a socially optimal choice, even if there is at least one choice that is both individually and socially optimal. A "controlling instance" that is "clearing the market" would still be needed to impose the choice that is both socially and individually optimal (for example by curtailing some of the production or not).

On the contrary, suppose now that everyone in a distribution network is facing the same real power price $\lambda$, which is for the moment a far more realistic assumption. Then the social optimum coming from solving (1.4.2) would most probably not result in an individual optimum for prosumer $i$, which would be obtained by solving (1.4.41) with $\lambda_i = \lambda$. Pricing real power uniformly at each node of a distribution network is ignoring the impact of position of the node in the network. Therefore, we are not taking into account the fact that line losses and network constraints can impact in a different way each node of the network (as we will see later in this thesis).

## 1.5 Conclusion of chapter 1

In this chapter, we presented a model to represent the optimal power flow problem on radial distribution networks with network constraints such as voltage control and line limits. From this non-convex model, we saw how by the mean of two successive relaxations, which are exact under some mild assumptions, we could obtain a SOCP model. Then, we performed a dual sensitivity analysis of the model. In particular, we highlighted the fact that if we want to properly represent the network constraints and give the right incentives to the prosumers to attain a socially optimal power flow, distribution locational marginal prices should be used. Indeed, they would be more appropriated that a generic electricity pricing common for every node of the network. It makes sense that the decentralization of the production and consumption of power should be accompanied with a decentralization of the pricing. In the reality, we are still far from that. Therefore, we need a control on consumption and injection in the distribution network, i.e. by curtailing re-injection, in order to ensure that line limits and voltage constraints are respected. In the next chapters, we will try to quantify the load curtailment and see to what extent it could be prevented by including storage possibilities in the network. To achieve that, we will first extend our OPF-SOCP problem in a multi-time-step OPF problem with storage investment possibilities.

# Chapter 2

# Multi-time-step OPF problem with energy storage capacity expansion

One of the main concerns coming from renewable energy sources is that the generation profiles have large fluctuations (e.g. wind or solar profiles). In a world with more and more distributed generation, there are also fluctuations in generation and demand profiles at the distribution level, due to households with photovoltaic panels (PV) and in a near future to electric vehicles (EV). In this context the questions of storage investment and of economical value of distributed storage arise.

Storage investment and capacity expansion implies that we develop a multi-time-step model. The size of the model will therefore grow extensively. Therefore, the fact that we have a SOCP model, which is more computationally tractable in comparison to a non-linear model, becomes even more relevant.

## 2.1 SOCP formulation of the problem

We aim to adapt our model (1.4.2)- (1.4.20) to allow for battery storage investment. We will now consider a multi-time-step OPF problem for an horizon of time $t \in \{1, 2, ..., T\}$. To model storage possibility, we will add the following variables,

- $e_{i,t}, \forall i \in \mathcal{N}, t \in \{1, ..., T+1\}$ : energy stored at node $i$ and time $t$.
- $f_i, \forall i \in \mathcal{N}$: storage investment/maximal storage capacity at node $i$.
- $p^{in}_{i,t}, \forall i \in \mathcal{N}, t \in \{1, ..., T\}$ : active power input to be stored at node $i$ and time $t$.
- $p^{out}_{i,t}, \forall i \in \mathcal{N}, t \in \{1, ..., T\}$ : active power output from the storage at node $i$ and time $t$.

We also have a set of constraints coordinating those new variables:

$$0 \leq e_{i,t} \leq f_i, \qquad \forall i \in \mathcal{N}, t \in \{1, ..., T\} \tag{2.1.1}$$

$$\underline{p^{in}_i} \leq p^{in}_{i,t} \leq \overline{p^{in}_i}, \qquad \forall i \in \mathcal{N}, t \in \{1, ..., T\} \tag{2.1.2}$$

$$\underline{p^{out}_i} \leq p^{out}_{i,t} \leq \overline{p^{out}_i}, \qquad \forall i \in \mathcal{N}, t \in \{1, ..., T\} \tag{2.1.3}$$

$$e_{i,t+1} = e_{i,t} + h(\xi^{in} p^{in}_{i,t} - \frac{1}{\xi^{out}} p^{out}_{i,t}), \qquad \forall i \in \mathcal{N}, t \in \{1, ..., T\} \tag{2.1.4}$$

$$e_{i,1} = 0, \qquad \forall i \in \mathcal{N}. \tag{2.1.5}$$

Constraint (2.1.1) states the capacity limits of the storage, constraints (2.1.2) and (2.1.3) are input/output power limits on the batteries, equation (2.1.4) describes the energy level in the storage at time $t+1$ based on the energy level at time $t$ and as function of the input and the output, where $\xi^{in}, \xi^{out}$ are respectively charging and discharging efficiency factor. Note that $h$ is the length of the time-step between $t$ and $t+1$. Since we will consider hourly time-steps in this work, we will drop the $h$ factor in the following, resulting in a small abuse of notation (mixing energy with power). Finally, we initialize the battery as empty at time 1 through constraint (2.1.5). In the same way, we could also impose to empty the battery at some time steps $t \in D \subseteq \{1, ..., T+1\}$ (e.g. in $t = 1$, $t = T+1$ or at the beginning of each new day/week/month).

Regarding the other variables, $P_i, Q_i, p_i^g, p_i^c, q_i^g, q_i^c, v_i, l_i$ we just need to define them for every time step, i.e. $P_{i,t}, Q_{i,t}, p_{i,t}^g, p_{i,t}^c, q_{i,t}^g, q_{i,t}^c, v_{i,t}, l_{i,t}$ and define constraints (1.4.3), (1.4.6)-(1.4.20) for every $t \in \{1, ..., T\}$. However active power balance constraints (1.4.4) (1.4.5) need to be slightly changed into :

$$p_{0,t}^{in} - p_{0,t}^{out} = p_{0,t}^g - p_{0,t}^c + \sum_{j \in C_0} (P_{j,t} - r_j l_{j,t}), \quad \forall t \in \{1, ..., T\} \tag{2.1.6}$$

$$P_i + p_{i,t}^{in} - p_{i,t}^{out} = p_{i,t}^g - p_{i,t}^c + \sum_{j \in C_i} (P_{j,t} - r_j l_{j,t}), \quad \forall i \in \mathcal{N}_+, \quad \forall t \in \{1, ..., T\}. \tag{2.1.7}$$

Finally, we need to add an investment cost term in the objective function,

$$\max \quad \sum_{i,t} C_i^c p_{i,t}^c - \sum_{i,t} C_i^g p_{i,t}^g - \sum_{i,t} I f_i, \tag{2.1.8}$$

where $I$ represent the cost of having 1 unit of storage available per unit of time, see section 3.2.4 to see how we can calculate that cost based on a fixed investment cost.

Finally, we can write our multi-time-step OPF problem as

$$(Primal): \quad \max \quad \sum_{i,t} C_i^c p_{i,t}^c - \sum_{i,t} C_i^g p_{i,t}^g - \sum_{i,t} If_i, \tag{2.1.9}$$

$$(\beta_{i,t}): \quad v_{A_{i,t}} = v_{i,t} - 2(r_i P_{i,t} + x_i Q_{i,t}) + (r_i^2 + x_i^2) l_{i,t}, \quad \forall i \in \mathcal{E}, \quad \forall t \in \{1, ..., T\} \tag{2.1.10}$$

$$(\lambda_{0,t}): \quad p_{0,t}^{in} - p_{0,t}^{out} = p_{0,t}^g - p_{0,t}^c + \sum_{j \in C_0} (P_{j,t} - r_j l_{j,t}), \quad \forall t \in \{1, ..., T\} \tag{2.1.11}$$

$$(\lambda_{i,t}): \quad P_{i,t} + p_{i,t}^{in} - p_{i,t}^{out} = p_{i,t}^g - p_{i,t}^c + \sum_{j \in C_i} (P_{j,t} - r_j l_{j,t}), \quad \forall i \in \mathcal{N}_+, \quad \forall t \in \{1, ..., T\} \tag{2.1.12}$$

$$(\mu_{0,t}): \quad 0 = q_{0,t}^g - q_{0,t}^c + \sum_{j \in C_0} (Q_{j,t} - x_j l_{j,t}), \quad \forall t \in \{1, ..., T\} \tag{2.1.13}$$

$$(\mu_{i,t}): \quad Q_{i,t} = q_{i,t}^g - q_{i,t}^c + \sum_{j \in C_i} (Q_{j,t} - x_j l_{j,t}), \quad \forall i \in \mathcal{N}_+, \quad \forall t \in \{1, ..., T\} \tag{2.1.14}$$

$$(\delta_{i,t}^{g+}): \quad p_{i,t}^g \leq \overline{p_{i,t}^g}, \quad \forall i \in \mathcal{N}, \quad \forall t \in \{1, ..., T\} \tag{2.1.15}$$

$$(\delta_{i,t}^{g-}): \quad \underline{p_{i,t}^g} \leq p_{i,t}^g, \quad \forall i \in \mathcal{N}, \quad \forall t \in \{1, ..., T\} \tag{2.1.16}$$

$$(\delta_{i,t}^{c+}): \quad p_{i,t}^c \leq \overline{p_{i,t}^c}, \quad \forall i \in \mathcal{N}, \quad \forall t \in \{1, ..., T\} \tag{2.1.17}$$

$$(\delta_{i,t}^{c-}): \quad \underline{p_{i,t}^c} \leq p_{i,t}^c, \quad \forall i \in \mathcal{N}, \quad \forall t \in \{1, ..., T\} \tag{2.1.18}$$

$$(\theta_{i,t}^{g+}): \quad q_{i,t}^g \leq \overline{q_{i,t}^g}, \quad \forall i \in \mathcal{N}, \quad \forall t \in \{1, ..., T\} \tag{2.1.19}$$

$$(\theta_{i,t}^{g-}): \quad \underline{q_{i,t}^g} \leq q_{i,t}^g, \quad \forall i \in \mathcal{N}, \quad \forall t \in \{1, ..., T\} \tag{2.1.20}$$

$$(\theta_{i,t}^{c+}): \quad q_{i,t}^c \leq \overline{q_{i,t}^c}, \quad \forall i \in \mathcal{N}, \quad \forall t \in \{1, ..., T\} \tag{2.1.21}$$

$$(\theta_{i,t}^{c-}): \quad \underline{p_{i,t}^c} \leq p_{i,t}^c, \quad \forall i \in \mathcal{N}, \quad \forall t \in \{1, ..., T\} \tag{2.1.22}$$

$$(\sigma_{i,t}^{+}): \quad v_{i,t} \leq \overline{v_i}, \quad \forall i \in \mathcal{N}, \quad \forall t \in \{1, ..., T\} \tag{2.1.23}$$

$$(\sigma_{i,t}^{-}): \quad \underline{v_i} \leq v_{i,t}, \quad \forall i \in \mathcal{N}, \quad \forall t \in \{1, ..., T\} \tag{2.1.24}$$

$$(\eta_{i,t}^{+}): \quad l_{i,t} \leq \overline{l_i}, \quad \forall i \in \mathcal{E}, \quad \forall t \in \{1, ..., T\} \tag{2.1.25}$$

$$(\eta_{i,t}^{-}): \quad 0 \leq l_{i,t}, \quad \forall i \in \mathcal{E}, \quad \forall t \in \{1, ..., T\} \tag{2.1.26}$$

$$\begin{pmatrix} \gamma_{1,i,t} \\ \gamma_{2,i,t} \\ \gamma_{3,i,t} \\ \gamma_{4,i,t} \end{pmatrix}: \quad \begin{pmatrix} v_{i,t} + l_{i,t} \\ v_{i,t} - l_{i,t} \\ 2P_{i,t} \\ 2Q_{i,t} \end{pmatrix} \in \mathbb{L}^3, \quad \forall i \in \mathcal{E}, \quad \forall t \in \{1, ..., T\} \tag{2.1.27}$$

$$(\tau_{i,t}^{+}): \quad e_{i,t} \leq f_i, \quad \forall i \in \mathcal{N}, \quad \forall t \in \{1, ..., T\} \tag{2.1.28}$$

$$(\tau_{i,t}^{-}): \quad 0 \leq e_{i,t}, \quad \forall i \in \mathcal{N}, \quad \forall t \in \{1, ..., T\} \tag{2.1.29}$$

$$(\delta_{i,t}^{in+}): \quad p_{i,t}^{in} \leq \overline{p_i^{in}}, \quad \forall i \in \mathcal{N}, \quad \forall t \in \{1, ..., T\} \tag{2.1.30}$$

$$(\delta_{i,t}^{in-}): \quad \underline{p_i^{in}} \leq p_{i,t}^{in}, \quad \forall i \in \mathcal{N}, \quad \forall t \in \{1, ..., T\} \tag{2.1.31}$$

$$(\delta_{i,t}^{out+}): \quad p_{i,t}^{out} \leq \overline{p_i^{out}}, \quad \forall i \in \mathcal{N}, \quad \forall t \in \{1, ..., T\} \tag{2.1.32}$$

$$(\delta_{i,t}^{out-}): \quad \underline{p_i^{out}} \leq p_{i,t}^{out}, \quad \forall i \in \mathcal{N}, \quad \forall t \in \{1, ..., T\} \tag{2.1.33}$$

$$(\kappa_{i,t}): \quad e_{i,t+1} = e_{i,t} + \xi^{in} p_{i,t}^{in} - \frac{1}{\xi^{out}} p_{i,t}^{out}, \quad \forall i \in \mathcal{N}, \quad \forall t \in \{1, ..., T\} \tag{2.1.34}$$

$$(\nu_i): \quad e_{i,1} = 0, \qquad \forall i \in \mathcal{N}. \tag{2.1.35}$$

Again we are here formulating a maximization problem to ease duality although in practice will rather use

$$\min \quad \sum_{i,t} C_i^g p_{i,t}^g - \sum_{i,t} C_i^c p_{i,t}^c + \sum_{i,t} I f_i, \tag{2.1.36}$$

as objective function. The only effect of this transformation is a change of sign of the objective value.

## 2.2 Dual formulation of the multi-time step OPF problem

The dual will then take the following form

$$
\begin{aligned}
(Dual): \min \quad & \sum_{i,t} (\overline{p^g_{i,t}}\delta^{g+}_{i,t} - \underline{p^g_{i,t}}\delta^{g-}_{i,t} + \overline{p^c_{i,t}}\delta^{c+}_{i,t} - \underline{p^c_{i,t}}\delta^{c-}_{i,t} && (2.2.1)\\
& + \overline{q^g_{i,t}}\theta^{g+}_{i,t} - \underline{q^g_{i,t}}\theta^{g-}_{i,t} + \overline{q^c_{i,t}}\theta^{c+}_{i,t} - \underline{q^c_{i,t}}\theta^{c-}_{i,t}) \\
& + \sum_{i,t} (\overline{v_i}\sigma^+_{i,t} - \underline{v_i}\sigma^-_i) \\
& + \sum_{i,t} \overline{l_{i,t}}\eta^+_{i,t} \\
& + \sum_{i,t} (\overline{p^{in}_i}\delta^{in+}_{i,t} - \underline{p^{in}_i}\delta^{in-}_{i,t} + \overline{p^{out}_i}\delta^{out+}_{i,t} - \underline{p^{out}_i}\delta^{out-}_{i,t})
\end{aligned}
$$

$$(P_{i,t}): \quad -2r_i\beta_{i,t} + \lambda_{i,t} - \lambda_{A_{i,t}} - 2\gamma_{3,i,t} = 0, \quad \forall i \in \mathcal{E}, \quad \forall t \in \{1,...,T\} \tag{2.2.2}$$

$$(Q_{i,t}): \quad -2x_i\beta_{i,t} + \mu_{i,t} - \mu_{A_{i,t}} - 2\gamma_{4,i,t} = 0, \quad \forall i \in \mathcal{E}, \quad \forall t \in \{1,...,T\} \tag{2.2.3}$$

$$(p^g_{i,t}): \quad -\lambda_{i,t} + (\delta^{g+}_{i,t} - \delta^{g-}_{i,t}) + C^g_i = 0, \quad \forall i \in \mathcal{N}, \quad \forall t \in \{1,...,T\} \tag{2.2.4}$$

$$(p^c_{i,t}): \quad \lambda_{i,t} + (\delta^{c+}_{i,t} - \delta^{c-}_{i,t}) - C^c_i = 0, \quad \forall i \in \mathcal{N}, \quad \forall t \in \{1,...,T\} \tag{2.2.5}$$

$$(q^g_{i,t}): \quad -\mu_{i,t} + (\theta^{g+}_{i,t} - \theta^{g-}_{i,t}) = 0, \quad \forall i \in \mathcal{N}, \quad \forall t \in \{1,...,T\} \tag{2.2.6}$$

$$(q^c_{i,t}): \quad \mu_{i,t} + (\theta^{c+}_{i,t} - \theta^{c-}_{i,t}) = 0, \quad \forall i \in \mathcal{N}, \quad \forall t \in \{1,...,T\} \tag{2.2.7}$$

$$(v_{i,t}): \quad \beta_{i,t} - \sum_{j \in C_i} \beta_{i,t} + (\sigma^+_{i,t} - \sigma^-_{i,t}) - \gamma_{1,i,t} - \gamma_{2,i,t} = 0, \quad \forall i \in \mathcal{N}_+, \quad \forall t \in \{1,...,T\} \tag{2.2.8}$$

$$(v_{0,t}): \quad -\sum_{j \in C_0} \beta_{j,t} + (\sigma^+_{0,t} - \sigma^-_{0,t}) = 0, \quad \forall t \in \{1,...,T\} \tag{2.2.9}$$

$$(l_{i,t}): \quad (r_i^2 + x_i^2)\beta_{i,t} + r_i\lambda_{A_{i,t}} + x_i\mu_{A_{i,t}} \tag{2.2.10}$$

$$+ (\eta^+_{i,t} - \eta^-_{i,t}) - \gamma_{1,i,t} + \gamma_{2,i,t} = 0, \quad \forall i \in \mathcal{E}, \quad \forall t \in \{1,...,T\} \tag{2.2.11}$$

$$(e_{i,t}): \quad \tau^+_{i,t} - \tau^-_{i,t} + \kappa_{i,t-1} - \kappa_{i,t} = 0, \quad \forall i \in \mathcal{N}, \quad \forall t \in \{2,...,T\} \tag{2.2.12}$$

$$(e_{i,1}): \quad \tau^+_{i,1} - \tau^-_{i,1} - \kappa_{i,1} + \nu_i = 0, \quad \forall i \in \mathcal{N} \tag{2.2.13}$$

$$(e_{i,T+1}): \quad \kappa_{i,T} = 0, \quad \forall i \in \mathcal{N} \tag{2.2.14}$$

$$(f_i): \quad \sum_t \tau^+_{i,t} = \sum_t I, \quad \forall i \in \mathcal{N}, \tag{2.2.15}$$

$$(p^{in}_{i,t}): \quad \lambda_{i,t} + (\delta^{in+}_{i,t} - \delta^{in+-}_{i,t}) - \xi^{in}\kappa_{i,t} = 0, \quad \forall i \in \mathcal{N}, \quad \forall t \in \{1,...,T\} \tag{2.2.16}$$

$$(p^{out}_{i,t}): \quad -\lambda_{i,t} + (\delta^{out+}_{i,t} - \delta^{out+-}_{i,t}) + \frac{1}{\xi^{out}}\kappa_{i,t} = 0, \quad \forall i \in \mathcal{N}, \quad \forall t \in \{1,...,T\} \tag{2.2.17}$$

$$\tau^+_{i,t}, \tau^-_{i,t}, \delta^{in+}_{i,t}, \delta^{in-}_{i,t}, \delta^{out+}_{i,t}, \delta^{out-}_{i,t} \geq 0, \quad \forall i \in \mathcal{N}, \quad \forall t \in \{1,...,T\} \tag{2.2.18}$$

$$\delta^{g+}_{i,t}, \delta^{g-}_{i,t}, \delta^{c+}_{i,t}, \delta^{c-}_{i,t}, \theta^{g+}_{i,t}, \theta^{g-}_{i,t}, \theta^{c+}_{i,t}, \theta^{c-}_{i,t}, \sigma^+_{i,t}, \sigma^-_{i,t} \geq 0, \quad \forall i \in \mathcal{N}, \quad \forall t \in \{1,...,T\} \tag{2.2.19}$$

$$\eta^+_{i,t}, \eta^-_{i,t} \geq 0, \quad \forall i \in \mathcal{E}, \quad \forall t \in \{1,...,T\} \tag{2.2.20}$$

$$\begin{pmatrix} \gamma_{1,i,t} \\ \gamma_{2,i,t} \\ \gamma_{3,i,t} \\ \gamma_{4,i,t} \end{pmatrix} \in \mathbb{L}^3, \quad \forall i \in \mathcal{E}, \quad \forall t \in \{1,...,T\}. \tag{2.2.21}$$

We will now try to give an interpretation to the new dual multipliers $\tau^+_{i,t}, \tau^-_{i,t}, \delta^{in+}_{i,t}, \delta^{in-}_{i,t}, \delta^{out+}_{i,t}, \delta^{out-}_{i,t}, \kappa_{i,t}, \nu_i$. In terms of sensitivity, $\tau^+_{i,t}$ can be seen as the marginal value of having one more unit of storage available at time $t$ and node $i$, $\delta^{in+}_{i,t}, \delta^{in-}_{i,t}, \delta^{out+}_{i,t}, \delta^{out-}_{i,t}$ are simply the marginal values of relaxing the input/output rates constraints in the batteries, $\kappa_{i,t}$ can be seen as the "price" or marginal value of one unit of energy stored in the battery, $\nu_i$ represents the effects of initializing the model with an empty storage.

Looking at (2.2.15), it is interesting to note that the total marginal investment cost for one node can be simply decomposed in the sum of the marginal values $\tau^+_{i,t}$ of having one more unit of storage available at each time step. Looking for non-zero values of $\tau^+_{i,t}$, we could identify which time-steps justify investment. If we write the KKT conditions corresponding to constraints (2.1.28)-(2.1.35) and the new variables, we have :

$$0 \leq f_i - e_{i,t} \perp \tau^+_{i,t} \geq 0, \qquad \forall i \in \mathcal{N}, \forall t \in \{1, ..., T\} \tag{2.2.22}$$

$$0 \leq e_{i,t} \perp \tau^-_{i,t} \geq 0, \qquad \forall i \in \mathcal{N}, \forall t \in \{1, ..., T\} \tag{2.2.23}$$

$$0 \leq \overline{p^{in}_i} - p^{in}_{i,t} \perp \delta^{in+}_{i,t} \geq 0, \qquad \forall i \in \mathcal{N}, \forall t \in \{1, ..., T\} \tag{2.2.24}$$

$$0 \leq p^{in}_{i,t} - \underline{p^{in}_i} \perp \delta^{in-}_{i,t} \geq 0, \qquad \forall i \in \mathcal{N}, \forall t \in \{1, ..., T\} \tag{2.2.25}$$

$$0 \leq \overline{p^{out}_i} - p^{out}_{i,t} \perp \delta^{out+}_{i,t} \geq 0, \qquad \forall i \in \mathcal{N}, \forall t \in \{1, ..., T\} \tag{2.2.26}$$

$$0 \leq p^{out}_{i,t} - \underline{p^{out}_i} \perp \delta^{out-}_{i,t} \geq 0, \qquad \forall i \in \mathcal{N}, \forall t \in \{1, ..., T\} \tag{2.2.27}$$

$$e_{i,t+1} = e_{i,t} + \xi^{in} p^{in}_{i,t} - \frac{1}{\xi^{out}} p^{out}_{i,t}, \qquad \forall i \in \mathcal{N}, \forall t \in \{1, ..., T\} \tag{2.2.28}$$

$$e_{i,1} = 0, \qquad \forall i \in \mathcal{N} \tag{2.2.29}$$

$$\tau^+_{i,t} - \tau^-_{i,t} + \kappa_{i,t-1} - \kappa_{i,t} = 0, \qquad \forall i \in \mathcal{N}, \forall t \in \{2, ..., T\} \tag{2.2.30}$$

$$\tau^+_{i,1} - \tau^-_{i,1} - \kappa_{i,1} + \nu_i = 0, \qquad \forall i \in \mathcal{N} \tag{2.2.31}$$

$$\kappa_{i,T} = 0, \qquad \forall i \in \mathcal{N} \tag{2.2.32}$$

$$\sum_t \tau^+_{i,t} = \sum_t I, \quad \forall i \in \mathcal{N}, \tag{2.2.33}$$

$$\lambda_{i,t} + (\delta^{in+}_{i,t} - \delta^{in-}_{i,t}) - \xi^{in} \kappa_{i,t} = 0, \qquad \forall i \in \mathcal{N}, \forall t \in \{1, ..., T\} \tag{2.2.34}$$

$$-\lambda_{i,t} + (\delta^{out+}_{i,t} - \delta^{out-}_{i,t}) + \frac{1}{\xi^{out}} \kappa_{i,t} = 0, \qquad \forall i \in \mathcal{N}, \forall t \in \{1, ..., T\} \tag{2.2.35}$$

We indeed see that the non-zero values of $\tau^+_{i,t}$ correspond to time-steps where $e_{i,t} = f$, i.e. the battery is charged at full capacity and there could be a marginal benefit of having more battery. If $e_{i,t} < f_i$ there is logically no marginal benefit of having more battery available ($\tau^+_{i,t} = 0$) since the battery is not even full.
In the case where the battery is only partially full, $0 < e_{i,t} < f_i$, we have $\tau^+_{i,t} = \tau^-_{i,t} = 0$ and (2.2.30) gives us $\kappa_{i,t-1} = \kappa_{i,t} = 0$ meaning that the marginal value of one unit stored in the battery will not change from previous time step unless we reach the limit of the battery. Note also than when $\tau^+_{i,t} > 0$, i.e. at time where $e_{i,t} = f_i > 0$, (2.2.23) gives us $\tau^-_{i,t} = 0$ and (2.2.30) becomes $\tau^+_{i,t} = \kappa_{i,t} - \kappa_{i,t-1}$. The marginal value of having one more unit of storage is the difference between the value of stored energy at two consecutive time steps. These values are being linked to locational marginal prices through equations (2.2.34) or (2.2.35). Therefore, there is a link between the values of $\tau^+_{i,t} > 0$ and the difference of locational marginal prices between two times steps.

Now consider an individual prosumer that has access to future locational marginal prices $\lambda_{i,t}$. For the sake of simplicity, suppose his generation and consumption are determined beforehand

by solving (1.4.41). Then his individual multi-time-step capacity expansion problem would be :

$$\max_{p_{i,t}^{in}, p_{i,t}^{out}} \quad \sum_t \lambda_{i,t}(p_{i,t}^{out} - p_{i,t}^{in}) - \sum_t I f_i \tag{2.2.36}$$

$$(\tau_{i,t}^{+}): \quad e_{i,t} \leq f_i, \qquad \forall t \in \{1, ..., T\} \tag{2.2.37}$$

$$(\tau_{i,t}^{-}): \quad 0 \leq e_{i,t}, \qquad \forall t \in \{1, ..., T\} \tag{2.2.38}$$

$$(\delta_{i,t}^{in+}): \quad p_{i,t}^{in} \leq \overline{p_i^{in}}, \qquad \forall t \in \{1, ..., T\} \tag{2.2.39}$$

$$(\delta_{i,t}^{in-}): \quad \underline{p_i^{in}} \leq p_{i,t}^{in}, \qquad \forall t \in \{1, ..., T\} \tag{2.2.40}$$

$$(\delta_{i,t}^{out+}): \quad p_{i,t}^{out} \leq \overline{p_i^{out}}, \qquad \forall t \in \{1, ..., T\} \tag{2.2.41}$$

$$(\delta_{i,t}^{out-}): \quad \underline{p_i^{out}} \leq p_{i,t}^{out}, \qquad \forall t \in \{1, ..., T\} \tag{2.2.42}$$

$$(\kappa_{i,t}): \quad e_{i,t+1} = e_{i,t} + \xi^{in} p_{i,t}^{in} - \frac{1}{\xi^{out}} p_{i,t}^{out}, \qquad \forall t \in \{1, ..., T\} \tag{2.2.43}$$

$$(\nu_i): \quad e_{i,1} = 0. \tag{2.2.44}$$

The KKT optimality conditions for this problem (2.2.36)-(2.2.44) exactly correspond to (2.2.22)-(2.2.35). So once again we can conclude that, if an individual prosumer was facing locational marginal prices, the socially optimal investment in battery would also be optimal for him. We can combine problem (1.4.41) with this problem (2.2.36), to obtain the general result that the social optimum (both for investment and dispatch) is also optimal for each individual prosumer facing distribution locational marginal prices.

## 2.3 Conclusion of Chapter 2

In this chapter, we have extended the model of chapter 1 into a multi-time-step problem with investment decision for storage. The problem grows in dimension but is still a SOCP problem, hence we can hope to solve it in reasonable amount time (depending on the size of the network and the number of time-steps of course), as we will do in next chapters. Through dual analysis, we saw that if we want social and individual optimum to coincide, individual prosumer should face locational marginal prices signal. Indeed, if we suppose that each prosumer has the same price signal, two similar prosumers at two different nodes of the network would have the same incentive to invest in the same amount of batteries. However, as we will see in chapter 4, the location in the network plays an important role in the socially optimal placement of the storage.

# Chapter 3

# A case study on a realistic European distribution network

We wish to test our model on a realistic distribution network, with real power consumption and high solar production from the households to assess different problematics:

- Identify voltage behavior in the network.
- Identify and quantify solar generation that is curtailed to prevent violating network limits.
- Identify if battery storage investment could be an economically viable way to (partially) tackle curtailment.
- Identify the optimal location of the storage along the line.
- Test the running time of our SOCP model on a multi-time-step investment problem.

## 3.1 Materials and data

The data we used in this thesis come from the data used in the PhD of Niels Leemput about "Grid supportive charging infrastructure for plug-in electric vehicles" [13]. The goal is to deal with data similar to a real distribution network. We will take the seasonal effects into account by running our simulation over 4 representative weeks of the year.

### 3.1.1 Distribution grid

We used a 29 households distribution network (figure 3.1), which is a slight simplification of a real urban feeder topology that was provided within the EIT-KIC InnoEnergy EVCity project [14]. The network is composed of one main feeder (primary lines, in red on the figure) and smaller lines connecting the households to the main feeder (secondary lines, in blue). Therefore, there are 29 households nodes, 29 connections nodes (between red and blue lines) and one substation node connection the low voltage network to a medium voltage network via a transformer of maximum power rating of 250 kVA. This gives us a total of 59 nodes. All households are assumed to be connected to the same phase, with a rated neutral-to-phase voltage of 230V.

As you can see on figure 3.1, the distance between the transformer and the first house is 350m. Then distance between two connection nodes on the main line is 7.2m until node 17 where there is a gap of 30m until the next house, after that connection nodes are 8.3m apart. The distance from each house to the main line (blue connection) is 10m. Therefore, every house is at a distance between 360 and 600m from the substation transformer. Characteristics for the two

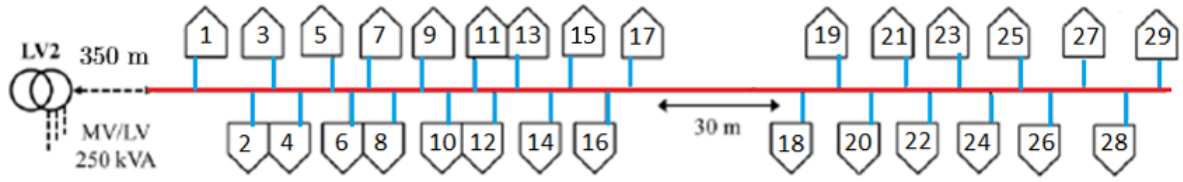


Figure 3.1: Schematic representation of the residential distribution network used

| Cable Type | Primary | Secondary |
|---|---|---|
| $Z^{cable}[\Omega/km]$ | 0.31+ 0.0713**i** | 1.15+ 0.083**i** |
| $I^{max}[A]$ | 210 | 120 |

Table 3.1: Characteristics of the lines of the distribution grid

types of lines can be found in table 3.1.

Note that in the rest of this work, we will use the following notations. Nodes on the main line will numbered from 0 to 29 while nodes corresponding to households will be numbered from 1bis to 29bis. Every line will take the name of his unique children. Therefore, red lines are labeled from 1 to 29 and blue lines from 1bis to 29bis. For example, the leftmost blue line on figure 3.1 is labeled 1bis and connects node 1 to node 1bis.

### 3.1.2 Residential load and solar generation profiles

We used 29 profiles of single-phase of households consumption with a resolution of one hour over 4 representative weeks of one year. The weeks are from different time of the year (February, May, August and November) to take seasonal effect into account. These data come from stochastically representative single-phase household electric power consumption profiles that were sampled in 2008 [13]. The profiles are identified as within an urban environment.

The PV power generation profiles are based upon measurement at an installations of the KU Leuven then scaled compared to the consumption of the households. A unity PF of 1 was assumed for the PV power generation.

In general, we will use 2 types of simulations. In the first one (case A), each household has his own different consumption and generation profiles. In the second one (case B), we will use the same consumption and generation profile for every household to identify phenomenons uniquely due to the position in the grid and to eliminate the impact of varying profiles. This common profile is the average of all 29 households profiles, which scaled to one year would correspond to an average consumption of ±2500 kWh/year and a production of ±1800 kWh/year per household.

## 3.2 Modeling assumptions and network constraints

### 3.2.1 Active power

We suppose each household with PV generation can produce (and re-inject in the grid) a fraction or the totality of his PV generation profile. In case of solar generation curtailment at one node (cannot produce at maximum capacity because of grid constraints), the production of solar is not completely shut down but reduced to an acceptable level, therefore the decentralized generation takes value in

$$0 \leq p_{i,t}^{g} \leq p_{i,t}^{solarmax}. \tag{3.2.1}$$

The curtailment is characterized as the solar energy that is not produced i.e.

$$curtailment = p_{i,t}^{solarmax} - p_{i,t}^{g}. \tag{3.2.2}$$

The substation transformer injects in the grid the rest of the necessary power to satisfy load at a certain cost but can also re-inject power at the same price in the medium voltage network if the decentralized generation is superior to the load.

### 3.2.2 Reactive Power

We will only focus on active power control in this thesis. First, we have only data for active power consumption, not for reactive power consumption and we assumed a power factor of 1 for PV generation. Furthermore, condition for exactness of the relaxation in theorem 1 states that we should allow for infinite reactive power consumption at each node, $\overline{q_i^c} = \infty$. Finally, reactive power control in radial distribution network (especially through the use of capacitors) has already been widely studied [15], [16], [17], [18]. Therefore, we will assume that reactive power is controlled independently, by allowing some reactive power generation/consumption at the substation as well as at each household (the bound on reactive generation is related to the amount of real power produced/consumed at this node) and we will focus on active power control.

### 3.2.3 Voltage control

Supply voltage should stay in a controlled range around the rated value (here 230 V) to ensure that electric devices can run normally and that the system is operated in a safe way. In [13], standards for voltage deviations are exposed. The European standard imposes to maintain the voltage in a +10%/-10% deviation range across the network. But since voltage variations appears through the entire system, only a fraction of the deviation is allowed to each voltage levels: high voltage, medium voltage and low voltage. The distribution system (low voltage) deviation margin in Flanders is stated to be -6%/+1.5%. Therefore, we impose the voltage $V_0$ at substation node to be constant and we allow for a this range of deviation of voltage across the line,

$$0.94V_0 \leq V_{i,t} \leq 1.015V_0, \tag{3.2.3}$$

or in terms of magnitude squared

$$(0.94)^2|V_0|^2 \leq v_{i,t} \leq (1.015)^2|V_0|^2. \tag{3.2.4}$$

### 3.2.4 Battery Storage Modeling

Typical costs for various storage technologies can be found in the literature, although the prices are changing quite fast. A detailed overview of different battery storages technologies, present and projected future prices, can for example be found in [19]. We will not enter in the details of the different technologies, but we will present the important parameters and how we can compute our investment price $I$.

The main parameters of a battery are :

- Storage capacity (kWh)

- Input/Output power limit (kW)
- Round-trip efficiency (%)
- Lifetime (cycles).

We suppose negligible dissipation rate in the battery. The lifetime is easily converted from cycles to years. For example, by assuming daily cycling, lifetime of 3000-4000 cycles corresponds to a lifetime of ±10 years. From the roundtrip efficiency, we have simply calculated

$$\xi^{in} = \xi^{out} = \sqrt{\eta}.$$

In theory, the total overnight cost (OC, cost to be paid upfront to buy the battery) of a battery can depend on all of 4 parameters listed above. But we will suppose we can invest in a certain amount of "battery cells", hence a certain capacity (in kWh) and that the other parameters are fixed or depend on this capacity.

**Example 1.** *A Tesla PowerWall 2 has the following characteristics:*

- *Storage capacity: 13.5 kWh*
- *Power max: 5kW*
- *Round trip efficiency: 89% (when in optimal conditions)*
- *Lifetime: 5000 cycles (± 13 years if daily cycled)*
- *Price: 5500 US$ (without installation costs).*

*If we imagine we can buy fraction/multiples PowerWall having the same characteristics, that would give us a total overnight cost of 364€/kWh, with $\eta = 89\%$, lifetime around 13 years and a maximum output that is around 37% (=5/13.5) of the storage capacity. This means it would take between 2 and 3 hours to fully (dis)charge the battery at maximum input/output rate.*

Inspired by example 1 above, we will change equations (2.1.30)-(2.1.33) of our model in:

$$p^{in}_{i,t} \leq 0.37 f_i, \tag{3.2.5}$$
$$0 \leq p^{in}_{i,t}, \tag{3.2.6}$$
$$p^{out}_{i,t} \leq 0.37 f_i, \tag{3.2.7}$$
$$0 \leq p^{out}_{i,t}, \tag{3.2.8}$$

where $f_i$ is the storage capacity of the battery. That means the ouput/input limit of the battery is 37 % of its capacity.

We will now to compute our hourly investment cost $I$ from an overnight cost OC, as it is done in [20]. From a total overnight cost, we can obtain an annualized fixed cost of investment given annual rate of discount $r$ as

$$FC = \frac{r \cdot OC}{1 - (1/1 + r)^T}. \tag{3.2.9}$$

We can further convert this yearly cost (FC, €/kWh/y) in an hourly cash flow. Indeed, dividing it by 8.76 we obtain our hourly investment cost $I$ (€/MWh/h).

**Example 2.** *Continuing with the example of the PowerWall, if we consider an overnight cost of OC= 364€/kWh, a lifetime of T= 13 years and annual rate of discount of 5%, we obtain a fixed investment cost of 38.75 €/kWh/y and I= 4.42 €/MWh/h, which would be the hourly price to pay to have 1 MWh of storage available.*

In a slightly optimistic point of view compared to what is actually done, we will use the following basis parameters in our model:

- Overnight Cost: 300 €/kWh
- Input/Output power limit: 37% of the storage capacity
- Round trip efficiency: 95%
- 10 years lifetime.

Note that following (3.2.9), this gives us an hourly price of $I = 4.435$ €/MWh/h which is very similar to the price computed in example 2. The most optimistic parameter being the roundtrip efficiency of 95% (and also the fact that we do not take installation costs into account).

Finally, we imposed batteries to be empty at the end of each week of simulations to not allow storing energy during summer week to be used later in winter week.

### 3.2.5 Objective function

The general formulation of the objective function in the simulations will be the minimization of a cost function

$$C(x) = \sum_{i,t} C_i^g p_{i,t}^g - \sum_{i,t} C_i^c p_{i,t}^c \tag{3.2.10}$$

or

$$C(x) = \sum_{i,t} C_i^g p_{i,t}^g - \sum_{i,t} C_i^c p_{i,t}^c + \sum_{i,t} I f_i, \tag{3.2.11}$$

in the case with investment in storage. From this general formulation will make a few assumptions to obtain the objective function we actually use in practice:

- We suppose the demand at each node is fixed, therefore the term $\sum_{i,t} C_i^c p_{i,t}^c$ becomes constant and is dropped out of the objective function.
- We suppose that what we optimize is the cost of power flow at substation node $\sum_t C_0^c p_{0,t}^g$. Since in case of overproduction, the distribution grid can re-inject in higher voltage grid, we allow $p_{0,t}^g$ to be negative. The cost of $C_0^g$ is then the price of energy at substation node which is fixed at 161.33 €/MWh from the network data we have. This seems slightly lower that current retail prices of power but we choose to keep it to stay coherent with our data set. Also, this price is roughly a scaling factor in the case without storage capacity expansion, the quantity we wish to minimize being the power consumed/re-injected at substation node $\sum_t p_{0,t}^g$. However, in case of storage investment, the ratio between $C_0^g$ and $I$ is determinant, as we will see in section 4.2.2.
- Although we suppose the generation cost of PV to be near 0, we still put a small cost $\epsilon_1$ to avoid strange numerical behavior and production that will be produced but not used (for example dissipated by charging and discharging the battery).

- We also add a small penalty on the sum of current $\epsilon_2 \sum_{i,t} l_{i,t}$ to make sure the optimal solution is a feasible solution, i.e. be sure that the relaxation is exact, see proposition 1 and remark 1. It is interesting to note that this penalty is needed. Without it, the solver outputs solution where the conic inequality is not exactly tight but it becomes tight with a correct penalty.
- The coefficient $\epsilon_1, \epsilon_2$ are tuned in order to have the solver behaving well but also not to impact too much the optimal solution. In practice, we took $\epsilon_1 = 0.01$ and $\epsilon_2 = 0.1$.

Our final objective function is therefore

$$C(x) = \sum_t C_0^g p_{0,t}^g + \epsilon_1 \sum_{i \neq 0,t} p_{i,t}^g + \epsilon_2 \sum_{i,t} l_{i,t} + \sum_{i,t} If_i. \tag{3.2.12}$$

## 3.3 Conclusion of Chapter 3

In this chapter, we presented data and modeling assumptions that were used to obtain results presented in the next chapter. We tried to be consistent to what could be a realistic network. A change of these data would of course impact the results of next chapter, although most important results are not numerical results but concerns the general behavior of the system.

# Chapter 4

# Results and analysis

## 4.1 Behavior without storage

First, we wish to investigate the behavior of the system in the case there are no storage investment possibilities. In order to do that we will begin with a non-voltage constraining simulation to try to understand the theoretical optimal behavior of the system when we do not constraint voltage magnitudes (except at substation node). Then we will observe the changes when the voltage constraint is enforced, which is the case in the reality. We will also assess the differences between having different profiles at each household or one common averaged one. Therefore, we have 4 different simulations results 1A, 1B, 2A, 2B with the following parameters significations:

- 1: Voltage constraint (3.2.4) not enforced
- 2: Voltage constraint (3.2.4) enforced
- A: Each household has its own consumption/production profile
- B: All households share the same consumption/production profile.

### 4.1.1 Without voltage constraint (case 1A and 1B)

#### Voltage behavior

First, we wish to observe how voltage would behave "naturally" if we do not impose any constraint on it. Figure 4.1 shows the averaged (over the 4 weeks) voltage profile across the 29 nodes of the main line. Voltages are expressed per unit of the value of voltage at substation node in order to better assess the variation through the line. This is the graph for case 1A, case 1B being very similar.

We see that, on average, the deviation from the nominal value is very small (less than 1%) and very far away from the bounds we will impose later (-6%/+1.5%). We also see the the voltage magnitude is on average decreasing across the line, with a dive between node 0 and node 1 due to the 350m of distance and then a smaller dive between nodes 17 and 18 due to the 30m separating them. Even if this give us an idea of the average behavior, this result is not very meaningful. There are indeed periodically much higher deviations of voltage, both over-voltage and under-voltage, which are counterbalancing themselves in this average. To make this appear let us look at the behavior of voltage at critical hours. Looking at figure 4.2, we can see voltage profiles for peak demand hour in February and for peak solar re-injection in May (case 1A, 1B is similar).

We notice that the two behaviors are very different and both would be breaking the voltage constraints. The effect of high demand is a drop of voltage along the line. Again we see that the main dive is between the substation node and node 1, after which voltage is decreasing steadily except for a small dive again between nodes 17 and 18. In the end, the maximum

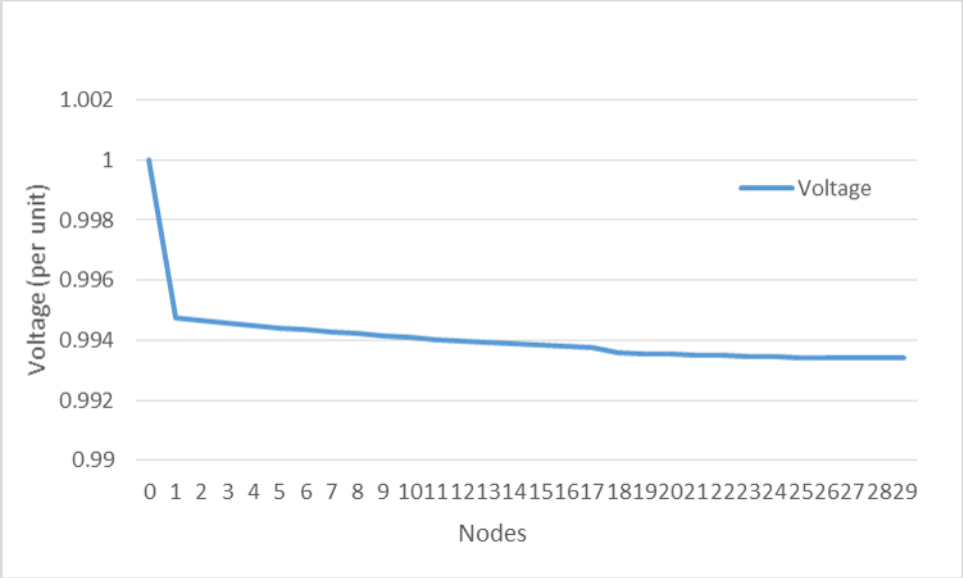


Figure 4.1: Average voltage behavior on the line (case 1A)

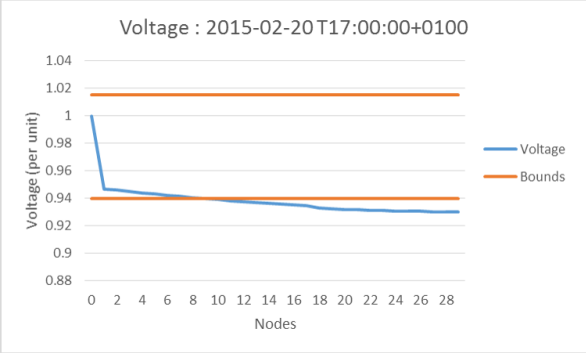


(a) Peak demand hour, February 20th, 17h

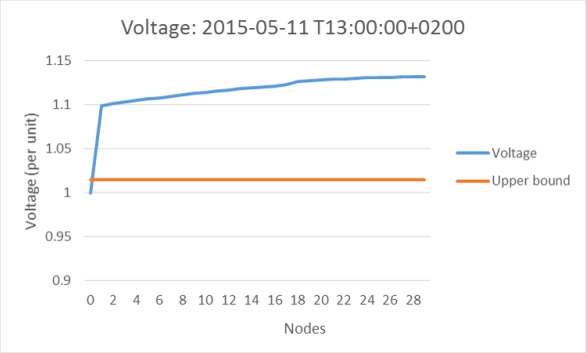


(b) Peak solar re-injection, May 11th, 13h

Figure 4.2: Voltage behavior across the line for critical hours (case 1A)

deviation reached is of the order of $-7\%$ compared to the nominal value. In case of massive solar generation, the production is superior to the demand and the power flows towards the substation where it is absorbed. The voltage behavior is opposite compared to peak demand, with jump at nodes 1 and 17 and a rather steadily increase elsewhere. The final voltage deviation is around $+13\%$ of the nominal value. The main conclusion we can draw from this first analysis is that high demand leads to under-voltage problems and high re-injection tend to lead to over-voltage issues. It also shows the interest of looking at critical hours instead of averaged profiles.

### Solar curtailment

Let us talk a bit about solar production curtailment. This happens when re-injecting more power in the network would cause to violate network constraints (voltage and/or line limits). We could imagine that in a case without voltage constraints, the curtailment phenomenon would not exist. In fact, as we can see at figure 4.3, there is still a small proportion of decentralized generation that is curtailed even if it is almost negligible ($<1\%$ of the maximal solar production). From curtailment graph in case 1A, we observe that the curtailment is located for production at the end of the line and is related to the maximal production of one household, the worst case being

a curtailment of the order of 7% for houses 28 bis and 29bis (there is much more solar capacity at house 28bis). When looking at case 1B, the effect of different solar capacity disappears and the effect of the position on the line appears clearly.

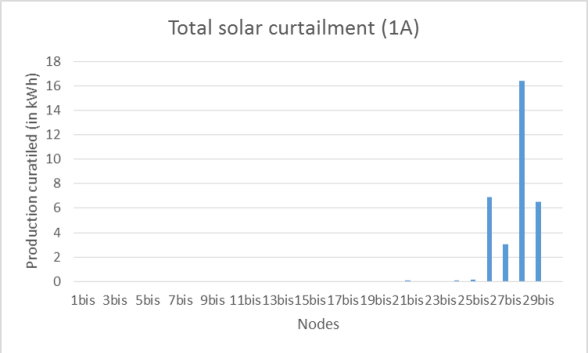


(a) 1A, curtailment at node 28bis and 29bis amount to ±7% of their production.

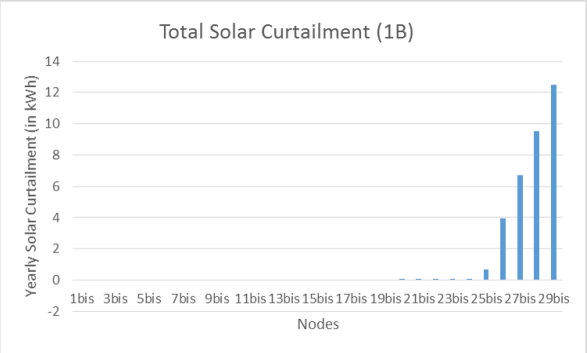


(b) 1B, curtailment at node 29bis amount to ±12% of his production

Figure 4.3: Total curtailment due to line limits, in both cases a total of ± 33kWh of solar are curtailed out of 4035kWh potential solar production (<1%).

Note that since we do not have voltage limits, this curtailment can only be due to line limits. Indeed, we can check that the constraint for current limit on line 1 is binding at some critical time-steps, leading to this curtailment.

#### Real lines losses

Since in the absence of voltage constraints, there is not a lot of real power lost due to solar curtailment, we could ask ourselves what is the amount of real power lost due to lines losses. Results for case 1A and 1B are very similar. Total line losses amounts to ± 470 kWh for the 4 weeks. In comparison, the total demand on the same period amounts to 5460 kWh and the solar production to 4030 kWh. Theses losses are decreasing along the main line, with more that 80% of the losses between node 0 and node 1 (due to the position but also to the 350m of length). To illustrate the effect of position only, we can compare the losses on line 2 and on line 17 which have similar characteristics. Losses are 4 times more important on line 2 that on line 17. Also note that losses on secondary (blue) lines are negligible (<1% in total).

These first results do not correspond to a realistic framework. Indeed, in practice voltage control is very important to ensure the correct operation of the system. However, this first case helps us to familiarize ourselves with the behavior of voltage, curtailment and line losses along the line. It also shows that enforcing voltage limits is necessary, as spontaneously the system would break both upper and lower bounds (see figure 4.2).

### 4.1.2 Realistic case with voltage constraints (case 2A and 2B)

We will now analyze the socially optimal operation of the system using a more accurate representation of an actual distribution network by restoring constraint (3.2.4). In this framework, we will conduct a similar analysis as above.

#### Voltage behavior

The voltage profiles have to be different than in the previous case, since they were breaking the bounds. However, on average we can see that the voltage is well inside the imposed bounds, see

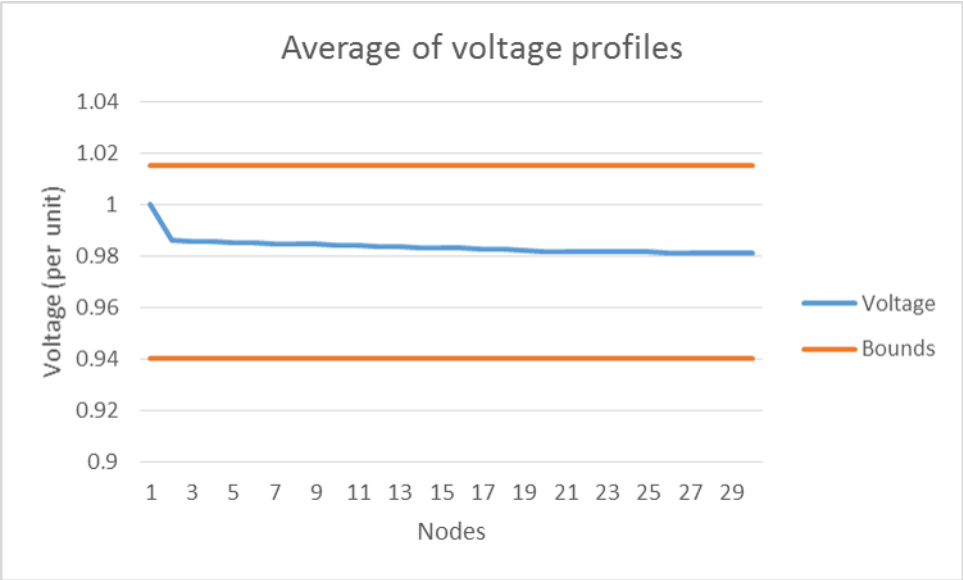


Figure 4.4: Average voltage behavior on the line (case 2A)

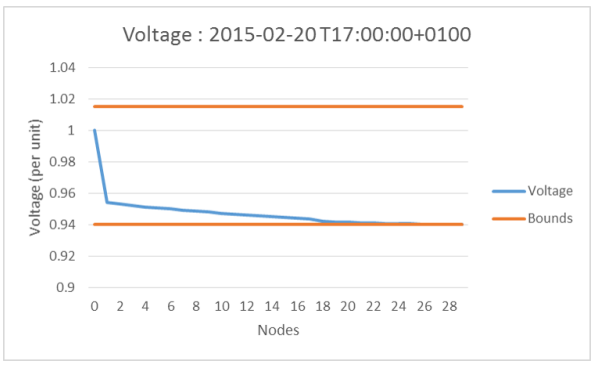


(a) Peak demand hour, February 20th, 17h

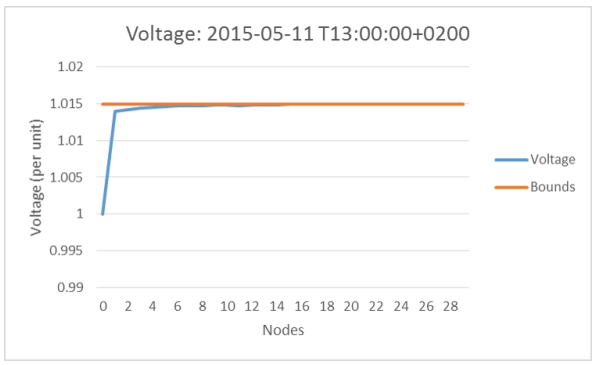


(b) Peak solar re-injection, May 11th, 13h

Figure 4.5: Voltage behavior along the line for critical hours (case 2A).

figure 4.4. This is for case 2A, profile for 2B is similar.

The most interesting result to take out this graph is probably that voltage tends to average in the middle of the two bounds (around 2% below the voltage at substation node). Again, we can make more interesting observations by looking at profiles for critical hours 4.5 (case 2A, 2B being similar).

For the peak demand hour, the voltage experiences a dive at first node then decreases steadily until reaching the lower limit. For high input of solar, the voltage almost immediately reaches the upper limit. Recall that without limits it was going up to +13% compared to the nominal voltage and we constrained it to +1.5 %, which leads to think a lot of curtailment took place in order to respect the constraint. This will be confirmed in next section.

Before that, we will look at the voltage profiles from a prosumer perspective. For that we consider the voltage profiles for an average consumer (case 2B) located at the beginning (1bis) and the end of the line (29bis). You can see the voltage profiles for a high solar re-injection day at figure 4.6.

We observe that the voltage is below the rated value when the demand is higher than the solar production (in the morning and in the evening) and that it jumps up to the upper bound when solar production is (well) superior to the demand. The only difference between being at

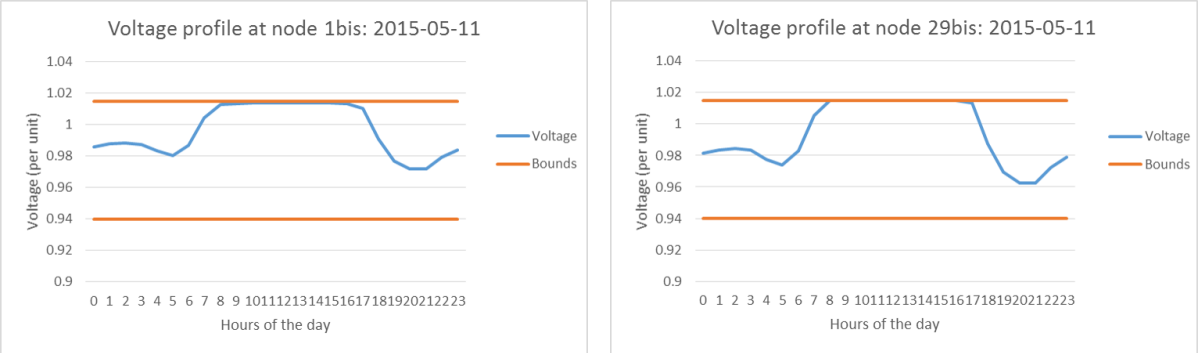


(a) Beginning of the line, node 1bis

(b) Enf of the line, node 29bis

Figure 4.6: Voltage profiles through a day of high solar production for an average consumer (case 2B)

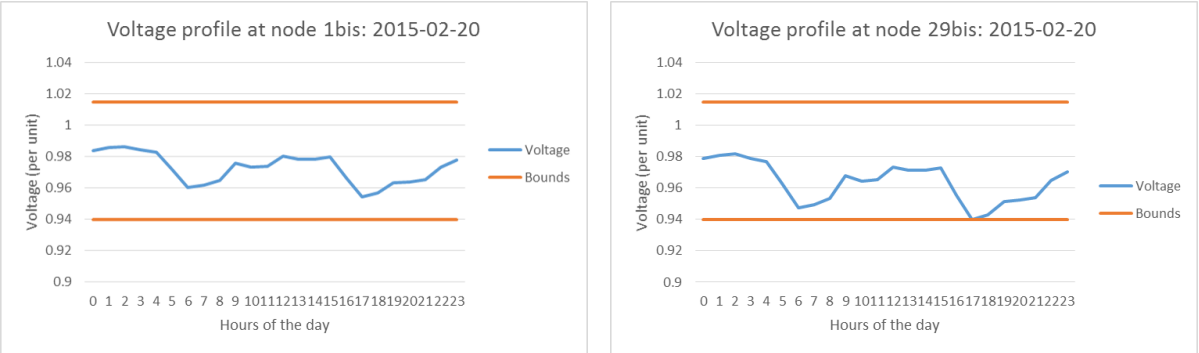


(a) Beginning of the line, node 1bis

(b) End of the line, node 29bis

Figure 4.7: Voltage profiles through a day of high demand an no solar production, for an average consumer (case 2A)

the beginning or at the end of the line is a bigger down-deviation in the evening. Indeed, in case of consumption of power, the voltage is lower in the end of the network. This is confirmed by looking at voltage profiles for a day with no solar production and high demand, figure 4.7. Since the demand profiles are the same for all houses, the voltage profiles are similar but the profile for the household at the end of the line is shifted down.

**Solar curtailment**

We have seen that the upper voltage limit is often reached in case of high solar generation. In that case, we should expect solar production to be curtailed to avoid over-voltage. We will first look at the curtailment for solar production at critical hour (whose voltage graph is at figure 4.5b), as a function of the total capacity of solar production, see figure 4.8a.

The first thing we can say is that logically, nodes with higher solar capacity should be more curtailed. But that is not the only determining factor as we see that production is way more heavily curtailed at the end of the line. This pattern will be confirmed by figure 4.9. From a certain node, solar production is even almost at 100% curtailed (there is very little demand at that time). Voltage limit is not the only reason to curtailment, line limits are also binding until node 4. Finally, note that the sum the power curtailed at this hour amounts to a total 35kW out of a total potential solar capacity of 55kW. That means that 63% of the possible production is curtailed !

This curtailment pattern is also reflected through the locational marginal prices profile, at figure 4.8b. Prices are going down along the lines and following curtailment pattern. As predicted through the analysis of the KKT conditions in Chapter 1, local prices go to 0 at nodes where solar power is curtailed (more precisely, they go to $\epsilon_1$, the marginal cost of solar production). Also note that the local prices at the time of high decentralized production are only a fraction of the price at substation node (161 €/MWh).

Of course this very high percentage of curtailment is for one of the critical hours, we will now look at the sum of curtailment through the 4 weeks of simulations. You can see results in case of varying profiles (case 2A, figure 4.9a) and an averaged household profile (case 2B, figure 4.9b).

Looking at figure 4.9b, we clearly see the impact of the position of the line on the curtailment. It is quite intuitive that households at the end of the line get curtailed first. Indeed, if the distributed generation in the network is superior to the demand, we wish to prioritize re-injection of the energy that is generated the closest from the substation node in order to minimize line losses. Although curtailment amounts to 80 % of its yearly production for house 29bis, it is not 100 %. First, there is always a part of the production that is used for auto-consumption (satisfy the demand of energy at the same time and location as production). Moreover, there are time-steps where solar generation is not too high and everyone can re-inject his overproduction. The rest of the production will most of the time be curtailed because other nodes are prioritized for re-injection and the network is already congestionned in terms of voltage and line limits. The problem is that hours of high demand (morning and evening) do not correspond with hours of high solar productions (middle of the day) so the auto-consumption phenomenon is limited. The connection to an electricity grid is supposed to allow not to loose the rest of the production. However, this case study shows us that in cases of high decentralized production, there will be a lot of curtailment due to to network constraints, up to 36 % of the total potential production in our case !

If we scaled the ± 1450 kWh losses on 4 weeks to a year, it would represent a yearly loss of ±19 MWh. If we ignored reality of the distribution network and we could theoretically sell this energy at our price of 161.33 €/MWh, it would represent a yearly loss of ± 3000 € for operating a 29 households network.

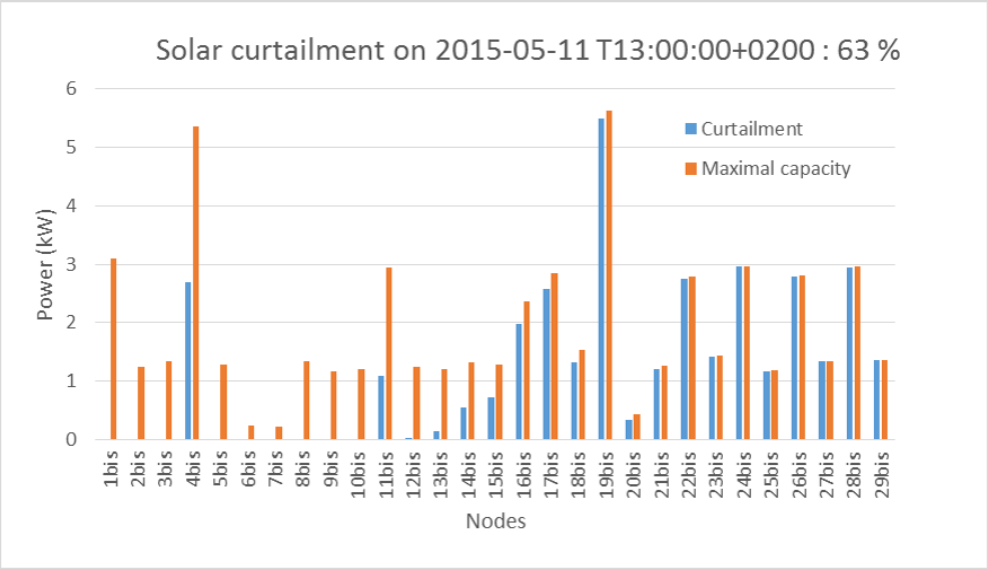


(a) Curtailment along the line

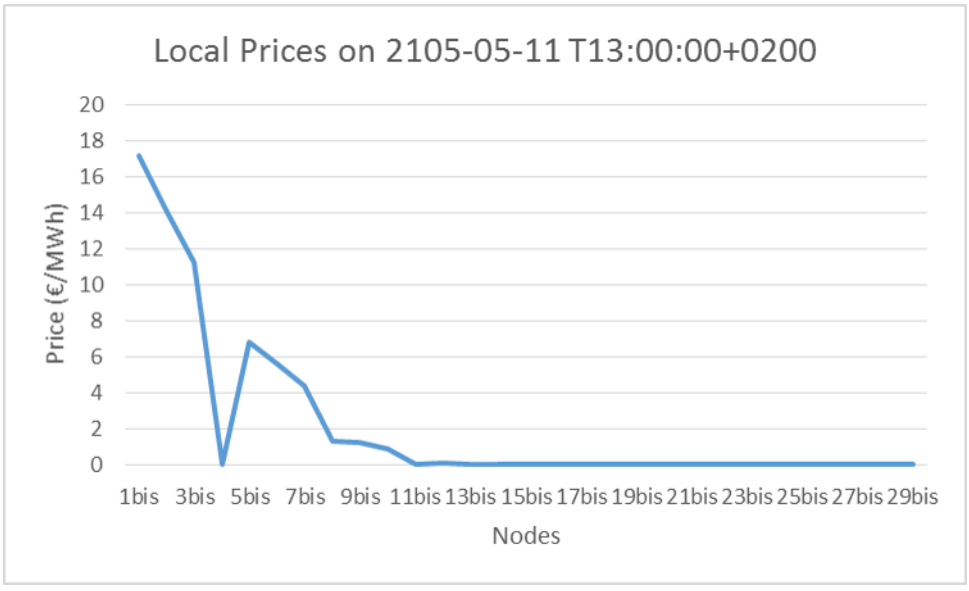


(b) Local Prices along the line

Figure 4.8: Curtailment behavior and local prices at peak solar hour, case 3A.

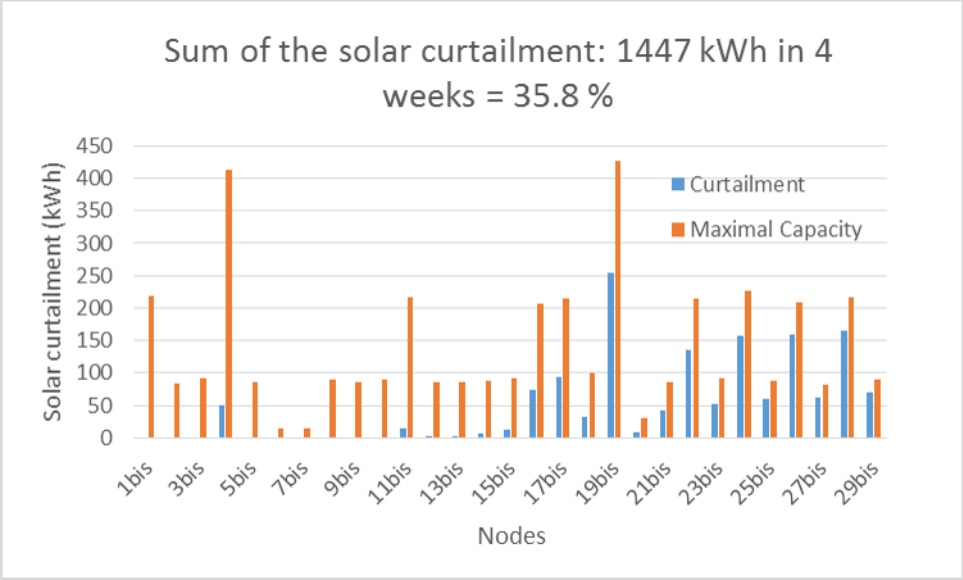


(a) Case 2A, different households profiles

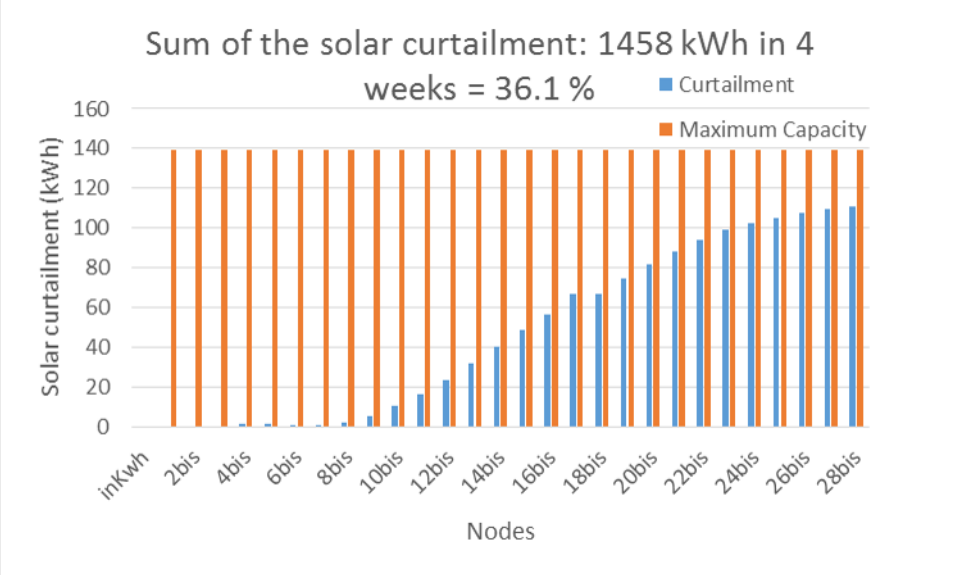


(b) Case 2B, common household profile

Figure 4.9: Total curtailment over 4 weeks per households compared to the capacity of production.

Finally, note that the losses due to curtailment are slightly superior in case of similar profiles (2B) than different ones (2A). That can be explained by the fact that in case 2A, at some time periods one house might be in overproduction (more than its consumption) while a neighboring house is consuming more than its production. Part of the overproduction of house 1 can then be consumed by house 2, without having to travel all the way to substation node to be re-injected in the medium voltage grid. In case of similar profiles, that cannot happen indeed if one house is in overproduction, they all are. Therefore, the only way to use the energy is to re-inject it all the way to the substation node.

#### Real Lines losses

We just checked the amount of active power loss due to solar curtailment. It might be interesting to make a comparison with the amount of active power that is lost in lines. Over the 4 weeks the amount of lines losses is 850 kWh for case 2A and 830kWh for case 2B. Scaled to one year this would represent a yearly loss of ± 11 MWh, or ± 1800 €. This is less than the loss due to curtailment but still quite substantial. The losses are mainly located on the first line (80 %) and on the rest of the main line. Losses on secondary lines represent ± 1% of the total losses.

### Local marginal prices

We have seen that local prices are varying as a function of the time and the place in the line. We wish to look at the average local prices along the line to see how we could price energy at each node. The idea would be to move closer to the social optimum thanks to a more elaborated pricing than a common price for each prosumer. We can see the yearly averaged price for each node at figure 4.10.

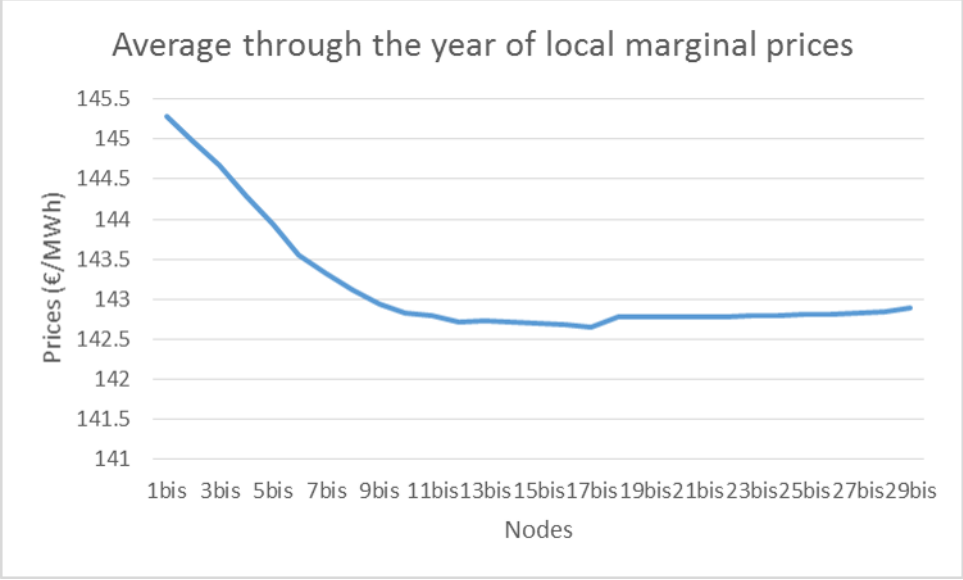


Figure 4.10: Average local prices on the line (case 2B)

As already illustrated at figure 4.8b, prices tend to decrease along the line. Note they are also under the marginal cost at substation node (161.33 €/MWh). However, we should be careful with these averaged prices because they result from the balance between two opposite behaviors as we can see at figure 4.11. In winter (figure 4.11a), when there is few solar production, the prices are at contrary increasing along the lines because the prosumers are consuming more than what we are re-injecting. Therefore, the power flows from substation to households and is more expensive at the end of the line. Note also that during the winter the prices are superior to the

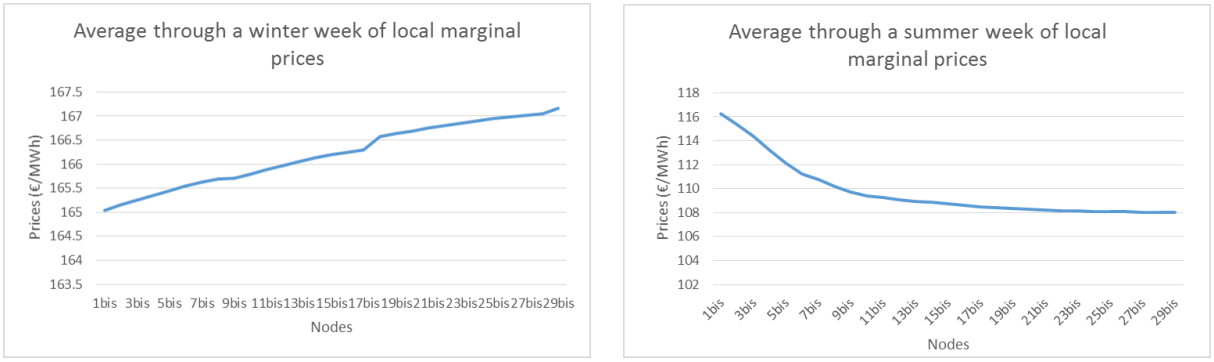


(a) Winter week

(b) Summer week

Figure 4.11: Total curtailment over 4 weeks per households compared to the capacity of production

marginal cost at substation node. In period of high solar production (figure 4.11b), the power flows in the opposite direction and therefore the price is lower at the end of the line.

This highlights the fact that if we want to achieve social optimum by correct incentive prices we should vary the retail prices of electricity as a function of the position in the line but also of the situation (case of consumption or case of overproduction). The ideal (though unrealistic) would of course be to price everyone at the real time locational marginal price.

### How to prevent the losses ?

We have just stated that correct price signals could be incentives for prosumers to behave in a socially optimal way. But before that, we have seen that even in a social optimum perspective, operating a system with a lot of decentralized production (the yearly solar production amounts to 73% of the total yearly consumption) leads to a lot of losses in the system, both due to solar curtailment and line losses.

Still from a social optimum point of view, we propose here 3 potential strategies to tackle those losses :

1. Optimize the solar capacity investment. An appropriate sizing and position of solar units could heavily decrease the curtailment phenomenon.

2. Invest in distribution lines. Indeed, increasing the capacity of lines would lead to a decrease of solar curtailment and decreasing their resistance would decrease real line losses.

3. Invest in battery energy storage. The goal is to balance the offset between peak consumption times and peak production times and therefore to support auto-consumption. This is the option we are considering in the next section.

## 4.2 Battery energy storage investment

We will now consider the problem where we allow investment for batteries storage as a way to improve the social optimum for operating the system (by decreasing line losses and/or solar curtailment). For this purpose, we use the model described in chapter 2 and the battery parameters described in 3.2.4. In particular, we wish to evaluate the economical interest and the optimal sizing and placement of batteries in different scenarios.

### 4.2.1 Base case (3A and 3B)

#### Optimal sizing and placement of batteries

First, we use the same framework as previously (case 2) with the same electricity pricing and a investment cost for batteries of 300 €/kWh (for start). We will again consider the case with different households profiles (case 3A) and the case with a common profile (case 3B). The optimal position and sizing of batteries in both cases can be seen at figure 4.12.

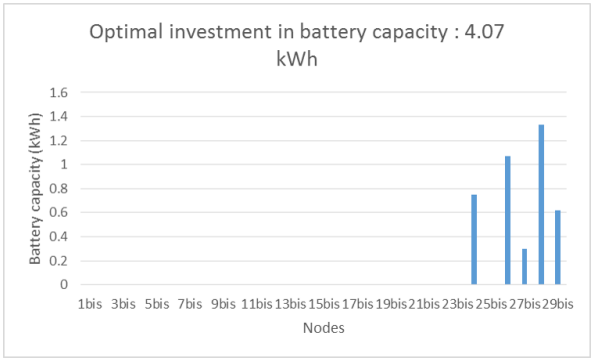


(a) Case 3A, different households profiles

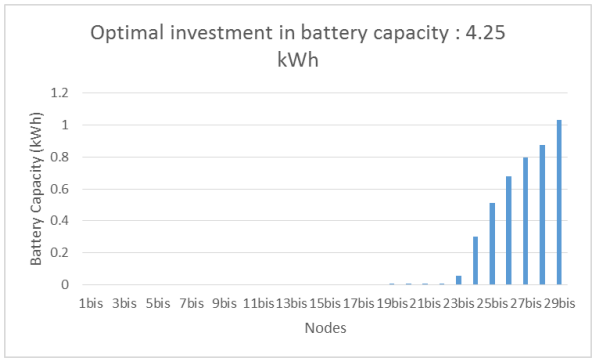


(b) Case 3B, common household profile

Figure 4.12: Optimal battery investment (Inv cost = 300€/kWh)

The first important result is that we should more heavily invest in batteries at the end of the line that in the beginning. Since nodes at the end of the lines are more heavily curtailed, it is quite logical that storage has more value at those nodes to try to store the production that is curtailed.

The second important result is that the optimal investment in battery is non-zero but very small. Summing optimal investment at all nodes, we reach a total of 4kWh of storage capacity (less than a single PowerWall). The effect on preventing curtailment and line losses is therefore also limited.

A summary of the main results until now is done at table 4.1. The results are for the 4 weeks time periods. To put numbers in perspective, the same results are presented with a yearly scaling (52 weeks) in table 4.2 and the main parameters are recalled in table 4.3.

We will first explain the small differences between case A and B. In case A, the curtailment is slightly less than in B because varying profiles make consuming solar production from neighbors possible. However, line losses are inferior in case B, probably because the averaged profile is "smoothing" the high demand hours for some locations and therefore tends to reduce slightly values of high current magnitude (losses are proportional to the square of current magnitude). In any case, the difference between case A and case B on the objective value is negligible. The interest of case B is to assess more precisely the effect of location on curtailment and battery investment.

Comparing case 1 and case 2 now, we see that voltage constraints have a huge impact on both curtailment and line losses which is also reflected in the objective value. However, comparing case 2 and case 3, we see that even if storage induce a small decrease in curtailment and losses, this small benefit is counterbalanced by the price of storage. Prices used are too high for the batteries to be actually valuable from a social optimum point of view.

| Case | Obj Value (€) | Curtailment (kWh) | Line Losses (kWh) | Stor Investment (kWh) |
|---|---|---|---|---|
| Case 1A | 315.35 | 32.97 (0.8%) | 471.67 | 0 |
| Case 1B | 314.82 | 33.41 (0.8%) | 468.51 | 0 |
| Case 2A | 608.28 | 1446.72 (35.8%) | 847.51 | 0 |
| Case 2B | 606.81 | 1458.32 (36.1%) | 829.83 | 0 |
| Case 3A | 607.70 | 1379.28 (34.1%) | 829.29 | 4.07 |
| Case 3B | 606.23 | 1387.84 (34.4%) | 811.26 | 4.25 |

Table 4.1: Main results for case 1 (without voltage constraints), case 2 (voltage constraints but no storage), case 3 (investment in storage is possible), for the 4 weeks of simulation. A=Different profiles, B=Common profile.

| Case | Obj Value (€) | Curtailment (MWh) | Line Losses (MWh) | Stor Investment (kWh) |
|---|---|---|---|---|
| Case 1A | 4100 | 0.42 (0.8%) | 6.13 | 0 |
| Case 1B | 4093 | 0.43 (0.8%) | 6.09 | 0 |
| Case 2A | 7907 | 18.81 (35.8%) | 11.02 | 0 |
| Case 2B | 7888 | 18.95 (36.1%) | 10.79 | 0 |
| Case 3A | 7900 | 17.93 (34.1%) | 10.78 | 4.07 |
| Case 3B | 7881 | 18.04 (34.4%) | 10.55 | 4.25 |

Table 4.2: Main results for case 1 (without voltage constraints), case 2 (voltage constraints but no storage), case 3 (investment in storage is possible), scaled to one year. A=Different profiles, B=Common profile.

| | |
|---|---|
| Number of households | 29 |
| Total demand over 4 weeks (MWh) | 5.46 |
| Total demand, scaled to a year (MWh) | 70.98 |
| Potential solar production over 4 weeks (MWh) | 4.03 |
| Potential solar production, scaled to a year (MWh) | 52.39 |
| Upper limit on voltage deviation | 1.5 % |
| Lower Limit on voltage deviation | -6 % |
| Real power price at substation node (€/MWh) | 161.33 |
| Storage investment price (€/kWh) | 300 |
| Storage investment price (€/MWh/h) | 0.44 |

Table 4.3: Main parameters used for cases 1,2,3.

**Effect of having a battery in the network**

We have just noticed that for the given prices, there is no justification for major investment in battery storage. Nevertheless, there is still around 4 kWh of battery that should be invested,

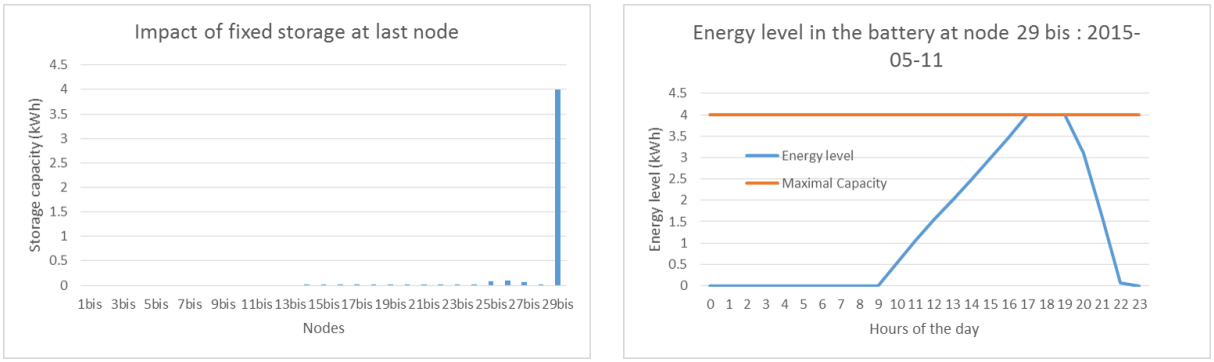


(a) Storage investment

(b) Energy level in the battery during one sunny day

Figure 4.13: Case 3B, but we fix 4 kWh of storage at node 29 bis.

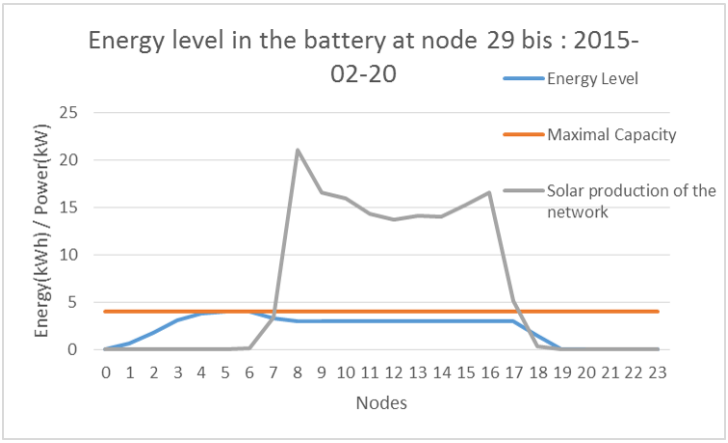


Figure 4.14: Energy level in the battery during one winter day compared to solar production of the whole network. Case 3B, but we fix 4 kWh storage at node 29 bis.

spread across the last nodes of the network. Following this result, we wish to invest in storage, but instead of having many small capacities of storage (<1 kWh), imagine we invest in a 4 kWh battery at last node. The question is to see the impact on optimal investment at other nodes, see figure 4.13a. We are also interested in the behavior of the battery, i.e. the level of energy that it is stored during the day, as shown in figure 4.13b.

The two graphs of figure 4.13 are rather intuitive. On the investment graph, we see that imposing battery at node 29bis cancels the incentive to invest at other nodes close to it. Looking at the graph on the right, we see that the battery is charging during the day, reaching his maximal capacity and then quickly discharges during the evening. We can verify that the hours of discharging (19-22) indeed correspond to peak demand hours.

The behavior of the battery at other times, especially in winter, is far less intuitive. You can see at figure 4.14, that not only the battery is used at his full capacity during a winter day but also that is fully charged at 5a.m. although no solar has been produced yet on the entire network (gray line on the graph) ! This means the prosumer has "bought" electricity all the way from the substation node to store it in the battery in order to reuse it later the same day. That is economically interesting because of the high variations of locational electricity price during the day (although price at substation node stays the same). This is confirmed by the graph of locational marginal prices for the same winter day at figure 4.15.

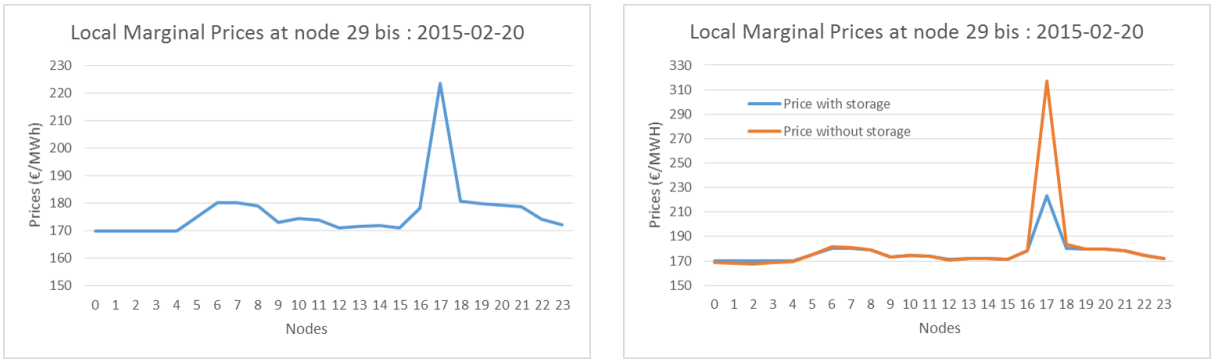


(a) Case 3B, but we fix 4 kWh storage at node 29 bis

(b) Comparison with price when there is no storage (case 2B)

Figure 4.15: Evolution of local marginal prices at node 29bis during one winter day.

On figure 4.15a, we see that there is a very high peak of local prices between 16h and 18h, i.e. when the demand is the highest. At that precise period, the battery is discharging and the consumer can use the electricity in order to avoid to pay the high local price. This phenomenon is due to the fact that we are considering social optimum which is equivalent to a situation where everyone is facing local marginal prices. Figure 4.15b, illustrates the effect of having a battery on the local marginal price by comparing it with local prices without the battery (case 2B in orange). We have seen that there was a peak at one period of time, but in fact this peak as already been reduced a lot. Therefore, we can say that batteries contribute to peak-shaving of locational marginal prices.

### 4.2.2 Impact of prices on optimal investment in batteries

In the previous section, we saw that although batteries can prevent curtailment, reduce some of the line losses and play a "peak-shaving" role on the local marginal prices, the current prices made the benefits not high enough compared to the investment cost, leading to very little storage investment. Does this mean that storage will never be a part of the distribution network ? A lot of research is being done in battery development and the interest in the topic is growing fast (batteries for electric vehicles, Solar City, ...) This growing interest is going together with a decrease of the technologies cost as we can see [19]. Hence, prices will most probably continue to decrease in a near future. The incentive for battery investment will therefore be higher. At figure 4.16, you can see the evolution of optimal investment in storage as a function of the decreasing investment cost. For example, if the overnight cost were to decrease to 200€/kWh (other parameters being equal), the optimal investment would amount to ± 50 kWh of capacity, more than 10 times the current optimal investment (4 kWh). Also note that the determining factor is the not really the investment price but rather the comparison between electricity price at substation node and investment price. In our case, we decided to fix the electricity price at the substation node and only make investment price vary.

## 4.3 "Off-grid" distribution network (e.g. island)

In this section, we examine a distribution network that is isolated, i.e. that is not connected to a medium/high voltage grid. Therefore, at the substation node we can only provide power to the distribution network, and we cannot absorb the overproduction of the decentralized generation. This situation can happen on an island or in any isolate location where we have a generator that supplies a few households without being connected to the national transmission network. In our

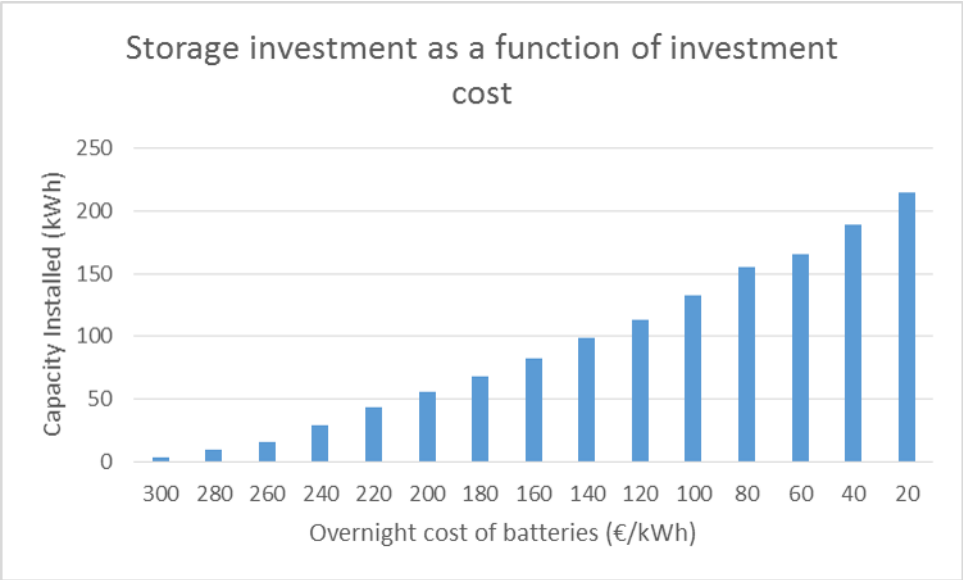


Figure 4.16: Evolution of optimal storage investment as a function of investment cost. Case 3A, case 3B is similar.

model, this can be represented by simply adding the constraint

$$p^g_{0,t} \geq 0 \qquad \forall t \in \{1, .., T\}. \tag{4.3.1}$$

However, note that the households can still re-inject in the distribution network in case there is another house in the network that could consume their overproduction. Nevertheless, since all houses have PV generation this phenomenon is very limited.

In this framework, the need for storage looks even more important. This will be confirmed by studying the curtailment in case with and without battery investment as before, we denote the new "island" cases as I2A, I2B, I3A, I3B.

Solar curtailment in case without battery investment (case 2) is represented at figure 4.17. We can see that almost all the solar production (98.6 %) is curtailed. The effect of the position in the line has no impact anymore since we cannot re-inject power all the way to the substation node. The only solar power that is actually used is used for auto-consumption. This also illustrates that given our dataset, the phenomenon of auto-consumption is limited to less than 2 % of the potential solar production. This is because hours of solar production (around 10h to 16h) coincides with hours of very low demand (people are usually not at home).

We may think that this almost full curtailment of the potential production should imply a very high incentive to have storage. You can see the optimal storage investment at figure 4.18.

First, note that for optimal battery investment, the position in the network still plays an important role. Indeed, by consuming power from the battery we are saving the transport of power from the substation to the location of the houses and we are therefore saving lines losses. From a social optimum point of view, if we were to place batteries, we should therefore place them at end of lines. The second observation is that the total battery capacity is around 8 times superior in the "island" case than in the "on-grid" case (31kWh against 4kWh). Even if this amount of storage becomes non-negligible and has a visible impact on the curtailment of solar production, the curtailment is only decreased by 15% as you can see on figure 4.19. We go from a curtailment of 98 % to a curtailment of 83 %, which is still disastrously huge.

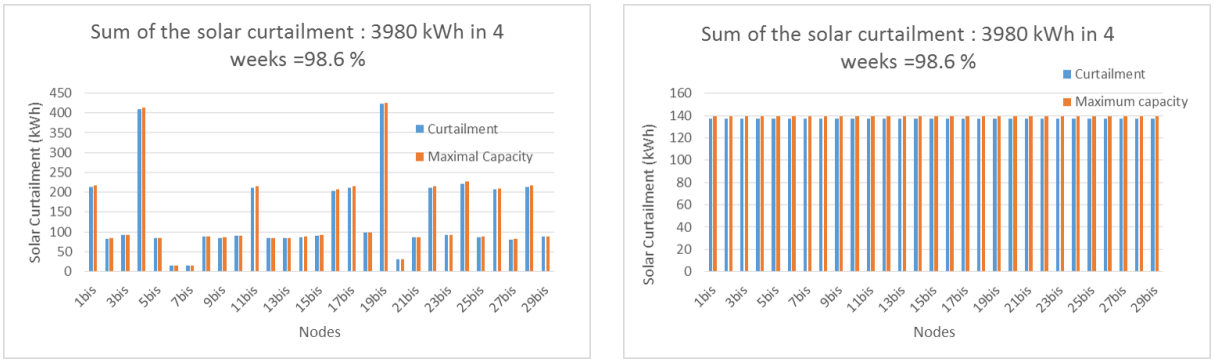


(a) Case I2A, different household profiles

(b) Case I2B, common household profile

Figure 4.17: Total curtailment per household over 4 weeks compared to the capacity of production, "island" case.

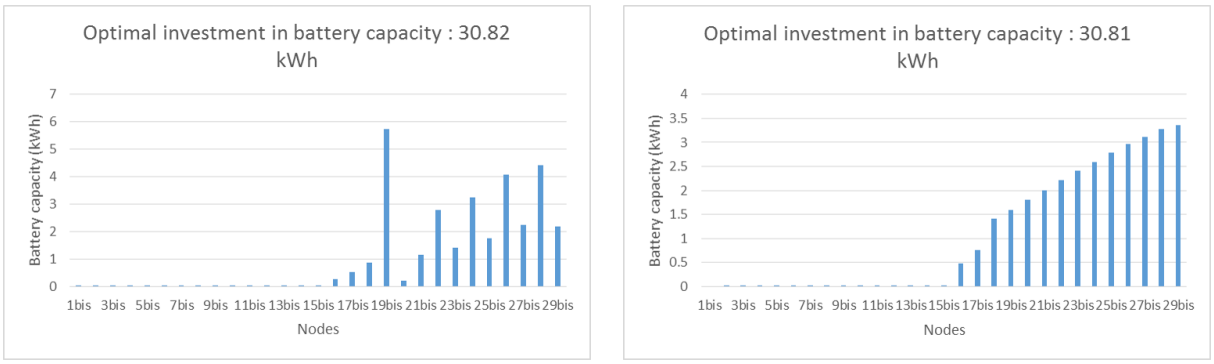


(a) Case I3A, different household profiles

(b) Case I3B, common household profile

Figure 4.18: Optimal battery investment in "island" case (Inv cost = 300€/kWh).

We could suppose that an isolated generator would have a production cost superior to the cost of power at the substation node of an "on-grid" network. That would make the investment cost smaller in comparison and the optimal investment in storage of course increases with decreasing investment price. The main conclusion is that it is not optimal to have such a large amount of solar production in a case where we cannot re-inject power in a larger network or store it at a cheaper price.

### 4.3.1 Comparison between centralized storage and decentralized storage

As a distribution network operator on an isolated network, we could propose to invest in batteries at the substation/generator node because we know there is solar generation in the network. Also, a centralized storage seems easier to implement (a lot of storage at one point) than decentralized storage. We will denote the "off-grid" case with centralized storage as case I4 ("off-grid" case with decentralized storage was case I3). Note that centralized storage at the substation node in a "connected to grid" model makes no sense except if we reach the transformer power rating limit (which was never the case in simulations 1,2,3).

Of course, centralized storage at the substation node is suboptimal as we have seen that storage should rather be placed in the end of the lines. We can verify that in case I4B the decentralized storage gives an optimal investment in storage of 14.5 kWh which is less than half the amount of optimal decentralized storage (case 3B).

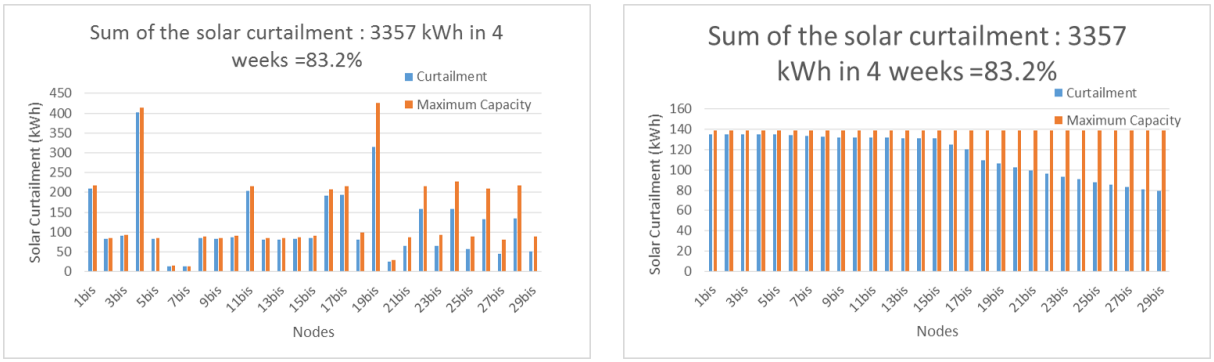


(a) Case I3A, different households profiles

(b) Case I3B, common household profile

Figure 4.19: Total curtailment over 4 weeks per household compared to the capacity of production, "island" case with storage.

| Case | Obj Value (€) | Curtailment (kWh) | Line Losses (kWh) | Stor Investment (kWh) |
|---|---|---|---|---|
| Case I2B | 903.75 | 3979.51 (98.6%) | 186.21 | 0 |
| Case I3B | 893.24 | 3357.36 (83.2%) | 137.06 | 30.81 |
| Case I4B | 898.48 | 3665.78 (90.6%) | 191.98 | 14.48 |

Table 4.4: Main results for case I2 (no storage), case I3 (investment in storage is possible), I4 (centralized storage only) for the 4 weeks of simulation. B=Common profile. I= "Island/Off-grid network".

The main numerical results for the off-grid cases are summarized in table 4.4. Since case A and case B are very similar (except for the localization of curtailment and storage), we only present the results for case B.

Comparing these results with table 4.1 highlights the high economical benefit of being connected to the transmission network.

## 4.4 Running time of the algorithm

The main reason to develop the SOCP relaxation of the AC-OPF problem is to get something that is computationally tractable. Indeed, a SOCP problem is convex and there exists methods and commercial solvers to solve these class of problems efficiently. In this thesis all codes were written using GAMS (General Algebraic Modeling System) and solved using Gurobi solver. All running times are given for Gurobi solver running on a portable computer.

In [21], a study about optimal storage investment on distributed network is also conducted. They solve a non-convex version of AC-OPF using various solvers. They show that the solving time grows exponentially with the size of the network. This implies that they cannot easily take the seasonal effect into account, being limited in time horizon. In [10], they develop a linearized multi-period optimal power flow method to tackle this problem. They also show that non-convex AC-OPF has an exponential running time. They also show running time of their method as a function of the simulation horizon. Interestingly enough, for the same horizon period (28 days with a 1 hour resolution time-step) their running times are similar to ours. Of course, the data and machines used to solve the problems are different but this illustrates that the SOCP clearly outperforms non-convex AC-OPF and can probably even be compared to some linearized methods in terms of running time.

| Time horizon (weeks) | Time-steps (=hours) | Running time |
|---|---|---|
| 4 | 672 | 33 sec |
| 8 | 1344 | 87 sec |
| 24 | 4032 | 226 sec |
| 32 | 5376 | 325 sec |

Table 4.5: Running time of multi-time-steps SOCP model with storage investment.

To further test the scalability of this model, we replicated noisy versions of our 4 weeks data and tested the model for longer horizons of time. Running times are reported in table 4.5. We could not simulate any horizon superior to 32 weeks because of the too few memory allowed to the program by our computer. Nevertheless, these running times clearly confirm the computational tractability of the model, as we could almost solve for a full year horizon with a one hour time-step resolution.

## 4.5 Conclusion of Chapter 4

In this chapter, we conducted various simulations based on the data presented in chapter 3. We first identified the natural behavior of not-constrained voltage. We noticed it would be violating deviation limits if not controlled. Then we showed that this voltage control enforcement can lead to a lot of PV production curtailment. As a logical next step, we tested the profitability of battery energy storage to tackle this phenomenon. Results show investment prices are currently still too prohibitive to lead to heavy investment of battery storage. Overproduction of PV panels can therefore not be entirely absorbed by storage nor by the network in a profitable way. This underlines the importance of having the appropriate amount of decentralized generation in the network. Last but not least, we validated that our model scaled well in size and could be used to solve capacity expansion for long horizons of time.

# Chapter 5

# Optimal investment from a prosumer point of view

All results of Chapter 4 were based on the hypothesis that we wish to achieve the social optimum. Therefore we presumed there was an instance solving an economic dispatch/capacity expansion problem and that everyone was behaving in order to achieve this social optimum. In this chapter however, we suppose each prosumer seeks to maximize his own personal benefit under different models of pricing. We will also allow consumers to invest in batteries. In an ideal world, the solution of each individual problem should lead to the social optimum behavior. We saw that this could be possible only if we had beforehand knowledge of the local prices at each nodes and each time-step. But this would require for example perfect forecast of solar production, future demand (or marginal benefit) of every prosumer, etc... which is hardly achievable in practice. Therefore, we will now present more realistic models of pricing and assess their impact on storage investment.

## 5.1 Uniform pricing

First, let us consider the most straightforward but still very applied model of pricing. The prosumer simply pays a uniform price for the power he consumes. In case of overproduction his electricity meter "turns backwards" and the network is buying him the power at the same price. The net power he is injecting in the network can be decomposed in his power generation minus his power consumption added to the eventual input/output of his battery. The constraints are very classical and lead to the following model :

$$\max_{p_t^{in},p_t^{out},p_t^g,p_t^c,f} \quad \sum_t \lambda(p_t^{out} - p_t^{in} + p_t^g - p_t^c) - \sum_t If \tag{5.1.1}$$

$$p_t^c = d_t, \qquad \forall t \in \{1,...,T\} \tag{5.1.2}$$

$$p_t^g \leq \overline{p_t^g}, \qquad \forall t \in \{1,...,T\} \tag{5.1.3}$$

$$0 \leq p_t^g, \qquad \forall t \in \{1,...,T\} \tag{5.1.4}$$

$$e_t \leq f, \qquad \forall t \in \{1,...,T\} \tag{5.1.5}$$

$$0 \leq e_t, \qquad \forall t \in \{1,...,T\} \tag{5.1.6}$$

$$p_t^{in} \leq \overline{p^{in}}, \qquad \forall t \in \{1,...,T\} \tag{5.1.7}$$

$$\underline{p^{in}} \leq p_t^{in}, \qquad \forall t \in \{1,...,T\} \tag{5.1.8}$$

$$p_t^{out} \leq \overline{p^{out}}, \qquad \forall t \in \{1,...,T\} \tag{5.1.9}$$

$$\underline{p^{out}} \leq p_t^{out}, \qquad \forall t \in \{1,...,T\} \tag{5.1.10}$$

$$e_{t+1} = e_t + \xi^{in} p_t^{in} - \frac{1}{\xi^{out}} p_t^{out}, \qquad \forall t \in \{1,...,T\} \tag{5.1.11}$$

$$e_1 = 0. \tag{5.1.12}$$

Note that since we assume the demand is fixed (no demand response), we could drop the demand term in the objective and simplify the model as

$$\max_{p_t^{in},p_t^{out},p_t^g,p_t,f} \quad \sum_t \lambda(p_t^{out} - p_t^{in} + p_t^g) - \sum_t If \tag{5.1.13}$$

$$(5.1.3) - (5.1.12). \tag{5.1.14}$$

This model, although still used, is not well-suited for distribution networks with high decentralized consumption. Indeed, it definitely does not take the network constraints into account. We suppose $\lambda > 0$, therefore the objective is strictly increasing in $p_t^g$ and the only constraint on production is (5.1.3). In this case, the optimal solution will always be to produce at he maximal amount of power and to re-inject in the network. If there are a lot of solars panel in the network, this will cause over-voltage and line limits problems as we have seen in the chapter 4. To avoid that, a mechanism should be put in place to force curtailment in case of stress on the network. Another consequence of that model, supposing we can always re-inject in the network is that we have no incentive to store energy at reuse it later. Therefore, the investment in batteries will always be zero (even if the batteries are very cheap). This model is advantaging the PV owner as the network is for him a "free storage". This is clearly not coming close to the social optimal solution in case of network with high decentralized production.

## 5.2 Day-Night Pricing

Another model that is widely used is a model with two different prices, more generally called "Time Of Use pricing' (TOU). The idea is to price the power higher at peak hours of demand and lower when the demand is very low. We sometimes call it "Day/Night" pricing, because peak hours generally correspond to day-hours and off-peak hours to night hours. If we denote $T_1$ and $T_2$ the set of hours where the price is respectively high ($\lambda_1$) and low ($\lambda_2$), we can write our model as

$$\max_{p_t^{in},p_t^{out},p_t^g,p_t^c,f} \quad \sum_{t\in T_1} \lambda_1(p_t^{out} - p_t^{in} + p_t^g - p_t^c) + \sum_{t\in T_2} \lambda_2(p_t^{out} - p_t^{in} + p_t^g - p_t^c) - \sum_t If \tag{5.2.1}$$

$$(5.1.2) - (5.1.12). \tag{5.2.2}$$

First, we note than once again it is optimal to produce at the maximum of the solar capacity and therefore we never reach as situation of curtailment. However, we might have an incentive to invest in batteries due to the two different prices. We could store energy when the price is low and sell/consume from the battery when the price is high. We can compute if such an arbitrage exists depending on the prices $\lambda_1, \lambda_2, I$ and the efficiency coefficients of the battery $\xi^{in}, \xi^{out}$.

Let us suppose $\lambda_1, \lambda_2, I$ are scaled to unity prices and we want to store 1 unit of energy in the battery. In this case, we need to buy from the network $\frac{1}{\xi^{in}} > 1$ energy unit, store it, in order to get an output of $\xi^{out} < 1$ energy unit. Note that the ratio energy output/energy input is $\xi^{out}\xi^{in} = \eta$, the efficiency rate of the battery. The gain of doing so is therefore

$$\xi^{out}\lambda_1 - \frac{1}{\xi^{in}}\lambda_2.$$

If the variation of price from $\lambda_2$ (when we can store energy) to $\lambda_1$ (when we can sell it) happens periodically every T' hour (and supposing we can ignore input/output limits), the operation is beneficial if the gain is greater than the cost of having one unit of battery available during this time, i.e. if

$$\xi^{out}\lambda_1 - \frac{1}{\xi^{in}}\lambda_2 > T'I. \tag{5.2.3}$$

**Example 3.** *In the data we received, the "Day-Night" pricing has the following characteristics: $\lambda_1 = 179.88$ €/MWh, $\lambda_2 = 137.38$ €/MWh, the day price $\lambda_1$ being used from 6h to 20h every day and $\lambda_2$ the rest of the time. We assume the same characteristics as presented in Chapter 3. Since both prices are used during more than 3 hours, we can ignore input/output power constraint because in 3h we can (dis)charge totally the battery. Therefore there is an arbitrage if*

$$\sqrt{0.95} \cdot 179.88 - \frac{1}{\sqrt{0.95}} 137.38 > 24I$$
$$34.38 > 24I.$$

*We see that with our investment price of $I = 4.44$ €/MWh/h, there is no arbitrage and that investing in battery is not beneficial. The investment price should be of $I = 1.4324$ €/MWh/h, which corresponds to an overnight cost of $\pm$ 97 €/KWh, in order to have an arbitrage.*

Such an arbitrage never exists in practice because it would require a very cheap storage and a big difference between $\lambda_1$ and $\lambda_2$. More important, if such arbitrage were to exist, the optimal investment would be to invest an infinite amount of storage in order to profit the most of the arbitrage. Since everyone can do the same reasoning, including the distributor of electricity, prices leading to such arbitrage will never exists. Therefore, we can conclude that as in the model with uniform pricing, the $Day - Night$ model does not take network constraints into account and never leads to investment in storage.

## 5.3 Prosumer pricing

In Flanders, there exists a pricing model called "prosumer" for prosumers willing to re-inject their overproduction in the grid. They pay a fee proportional to their maximum re-injection in the grid. If we consider the price $P$ (€/MW/h) for the maximum re-injection, we have the following model

$$\max_{p_t^{in},p_t^{out},p_t^g,p_t^c,f,p^{max}} \quad \sum_t \lambda(p_t^{out} - p_t^{in} + p_t^g - p_t^c) - \sum_t If - \sum_t Pp^{max} \tag{5.3.1}$$

$$p_t^{out} - p_t^{in} + p_t^g - p_t^c \leq p^{max}, \qquad \forall t \in \{1, ..., T\} \tag{5.3.2}$$

$$0 \leq p^{max} \tag{5.3.3}$$

$$(5.1.2) - (5.1.12). \tag{5.3.4}$$

Compared to the two previous models, we now probably do not always want to output the maximum of our solar generation, since it may increase our maximum net injection in the network $p^{max}$ and therefore decrease our total benefit. If the price $P$ is high enough, it may leads to "self-curtailment" or investment in batteries. Common values for $P$ used in Flanders are around 100 €/kW/year, if we divide it by 8.76 we obtain a price of $P = 11.42$ €/MW/h.

Using the same demand and PV profiles as in Chapter 4, we can verify that this model would indeed lead to curtailment, see figure 5.1 (again for cases A and B).

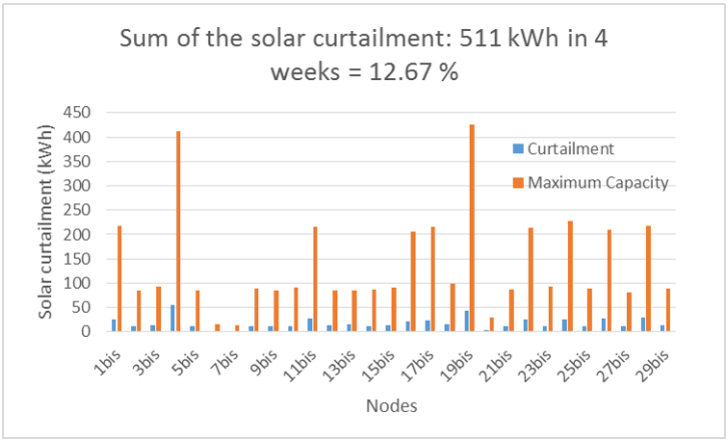


(a) Case 2A, different households profiles

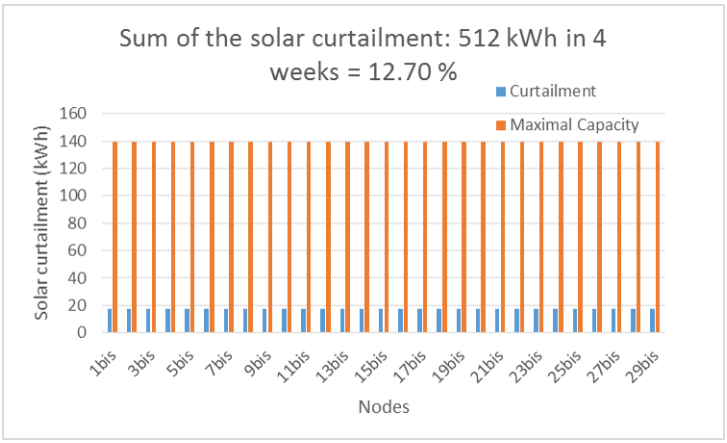


(b) Case 2B, common household profile

Figure 5.1: Total curtailment over 4 weeks compared to the capacity of production in the case of "Prosumer Pricing".

With this pricing, the curtailment is far less than in figure 4.9 which was the optimal curtailment from a social point of view. Moreover the investment in battery is zero for both cases although it was around 4kWh in the social optimum (see figure 4.12). More importantly

the effect of the position of the line as of course disappeared since everyone is facing the same pricing.

We could ask ourselves if this dispatch would lead to a feasible (suboptimal) solution of operating the network. We can do that by using the results we just obtained to fix power generation and battery investment in the model of chapter 2, then try to solve the resulting OPF problem. As we could have guessed, this results in a non-solvable instance of the problem, because the solar re-injection is too high, making voltage constraints impossible to satisfy. If we were dropping the voltage constraints, we would obtain deviations of $-8\%$ / $+8\%$ compared to the rated voltage. This would violate the voltage range that we wish to maintain in our network (-6 %/ +1.5 %) This can be explained by the fact that current prices are probably not designed for so much decentralized production. We can verify that by increasing the price $P$,

1. We reach solutions (with more curtailment) that are feasible for the OPF problem.
2. For high $P$, there is incentive to invest in some storage capacity.

Note that "Uniform Pricing" and "Day-Night Pricing" never result in a feasible OPF solution since the production of solar is always pushed to its maximum. Therefore, we could argue that this solution is better that the previous ones and come closer to social optimum for a right choice of $\lambda, P$. However, this solution carries still some flaws since it does not take the position of the house in the network into account although we have shown that it plays a role in both optimal curtailment and optimal storage investment. It also does not make the price of power vary as a function of the state of the network (high production/high demand) although this is also a very important factor.

## 5.4 Bidirectional Pricing

Another way of pricing that as been recently implemented and will for example be implemented in Brussels area as from 1st January of 2018 is "bidirectional pricing". By that, we mean that the prosumer as a bidirectional meter with a counter for input and one counter for output. The goal is to price separately the power that he consumes from the network and the power he injects in the network. Let us denote $\lambda_1$ the price of consuming power and $\lambda_2$ the price of re-injecting power (usually $\lambda_1 > \lambda_2$). Then our model can be expressed as

$$\max_{p_t^{in}, p_t^{out}, p_t^g, p_t^c, f} \quad \sum_t \lambda_2 \max(0, p_t^{net}) - \sum_t \lambda_1 \max(0, -p_t^{net}) - \sum_t If \tag{5.4.1}$$

$$p_t^{net} = p_t^{out} - p_t^{in} + p_t^g - p_t^c \qquad \forall t \in \{1, ..., T\} \tag{5.4.2}$$

$$(5.1.2) - (5.1.12). \tag{5.4.3}$$

First note that as uniform and day/night pricing there is no incentive to ever curtail the production. However, the difference between $lambda_1$ and $lambda_2$ is an incentive to auto-consume and therefore can be an incentive to invest in batteries (and also maybe to adjust his solar capacity to his consumption).

We could try to reason as we did for Day/Pricing to see whenever investment in storage is beneficial. Let us imagine, that we decide to store 1 unit of energy in the battery from time of overproduction to time of consumption. The value of this unit before being stored is $\frac{1}{\xi^{in}}\lambda_2$ and the value once it is out of the battery is $\xi^{out}\lambda_1$. Hence, the gain is

$$\xi^{out}\lambda_1 - \frac{1}{\xi^{in}}\lambda_2.$$

However, unlike in the day/night pricing, we can hardly suppose that this switch of prices happens periodically, during the same time every day and "overproducing" the same amount of power. Therefore, we cannot easily define the investment cost that should be compared to this gain. But we could probably make some estimations without having to solve the problem.

**Example 4.** *Suppose there is one overproduction "block of hours" per day (e.g. between 10h and 16h) and that your overproduction per day goes from 0 to 10kWh with an average of 5kWh. Therefore we suppose you have a 10kWh battery. Then we could estimate that batteries would be economically interesting if*

$$5 \cdot (\xi^{out}\lambda_1 - \frac{1}{\xi^{in}}\lambda_2) > 24 \cdot 10I,$$

*where $\lambda_1, \lambda_2$ are given by the distribution operator and would be in €/kWh, while I would be in €/kWh/h.*

Note also that in this problem, the same good (real power at instant t) is traded at different prices depending if we buy it or if we sell it, which is economically unusual. We could indeed claim that the distributor is charging too much his clients because he is making profit out of the difference of price. Especially in a case with few PV producers and a system running far far of its limits, the prosumer with PV could feel "cheated" by the distribution grid operator as it is illustrated in the following example.

**Example 5.** *Suppose houses A and B are so close that we can neglect the small line losses between them. Suppose that house A has PV panel and the house B has not and suppose further $\lambda_1 = 0.15$ €/kWh and $\lambda_2 = 0.10$ €/kWh. During a sunny hour, the prosumer A will sell 1 extra kWh he is overproducing to the network for* 0.10 €*. Meanwhile, house B is paying* 0.15 *to consume 1 kWh from the network (which was in fact produced by A). Therefore the distribution network operator as won* 0.05 € *(or a bit less because of losses) by buying and selling same product at different prices at the same time and almost same place. If A noticed that phenomenon, he could propose to B to "buy" power directly from its place (e.g. by plugging in at his place) at* 0.15 €/kWh *to retrieve the* 0.05 € *for himself. In this case, everyone is paying (or receiving)* 0.15 € *for a kWh of power. This works until the moment A is overproducing a kWh but B does not need to consume it, i.e. when the whole system (composed here of two houses) is in overproduction.*

Example 5 can seem a bit fabricated and not realistic since it is not easy to trade power without using distribution network. Nevertheless, it illustrates the fact that at same location and same time, a same commodity should probably bought and sold at the same price.

## 5.5 Conclusion of Chapter 5

This list of models for power pricing is not exhaustive as there exists many other models/variations of those models. In practice, there are also extra costs such as a yearly fixed cost of using the grid. Pricing of power in distribution networks is currently a very hot topic and the legislation is varying with time and countries. Each country has almost his own specific way of pricing. In Belgium alone, there are differences between Flanders, Wallonie or Brussels. Nevertheless, the 4 models above present the main ideas of the tariffs used in Belgium, each of them having its own specificities and flaws. Note also that to the best of our knowledge, no existing model makes a differentiation in pricing as a function of the consumer position in the network.

# Extensions

## Capacity expansion on PV panels

As we have seen in Chapter 4, battery storage at current prices are not profitable enough to tackle the problem of solar generation curtailment. We have also seen that PV production is more curtailed at the end of the line than at the beginning of the line. We could therefore adapt our model to optimize not only the size and placement of storage but also to optimize the size and placement of solar panels.

For that, we will assume we know the PV generation profile for the equivalent of one "unit" of PV panel (one unit can be defined as one solar panel or one solar cell). We also suppose that at each time-step a solar unit can produce an amount up to $p_t^{solarmax}$ which is the given solar profile. We introduce the decision variable $s_i$ as the amount of solar units household $i$ has. We make the assumption that we can have fractions and multiple solar units, so that $s_i$ can take any positive continuous value such that

$$0 \leq s_i \leq \overline{s_i}, \quad \forall i \in \mathcal{N}_+. \tag{5.5.1}$$

It is also reasonable to put an upper bound $\overline{s_i}$ on the amount of solar units a household can have, this can for example depend on the rooftop surface. Similarly to what is done for battery investment price in section 3.2.4, from an overnight cost for a solar unit (€/p.u.) and a lifetime, we can compute an hourly investment cost $I_2$ (€/p.u./h). The objective function in its minimization form becomes

$$\min \quad \sum_{i,t} C_i^g p_{i,t}^g - \sum_{i,t} C_i^c p_{i,t}^c + \sum_{i,t} I f_i + \sum_{i,t} I_2 s_i. \tag{5.5.2}$$

Concerning the constraints, we just need to add constraint 5.5.1 to the model and modify constraint on power generation as

$$0 \leq p_{i,t}^{gen} \leq s_i p_t^{solarmax}. \tag{5.5.3}$$

Note that the model keeps his convexity property and that we could choose to optimize only solar investment or both solar and battery investment. Note that even if beforehand optimizing of PV sizing would most probably reduce PV curtailment, it is not likely to kill it totally. Indeed, the offset between high production time and high consumption time is still present. It could be interesting to invest in PV capacity even if we know it will be partially curtailed for a small proportion of time. In this context, co-optimization of both PV and storage investment seems relevant.

## Capacity expansion on the lines

The most natural way of reducing curtailment and line losses would probably be to expand distribution network lines. However, this is costly and not easy to implement in practice (as lines are often underground). The second challenge is that we cannot extend our SOCP model to integrate capacity extension on the lines as easily as we did for PV panels.

The effect of replacing line with bigger lines or adding parallel lines is to decrease the impedance of the line $i$ considered. Considering impedances as new decision variables would lead the problem to loose its SOCP property, because impedances are multiplied with other decisions variables (current and power).

If we still want to assess the effect of expanding lines, we should probably define possible scenarios of extensions, solve the SOCP model for each and compare the results. This solving by enumeration is possible if

- We are working with instances of the problem where SOCP model runs relatively fast like it was the case for our simulation.
- We limit the numbers of scenarios we have.

Interesting scenarios could be

- Expand every line by a certain percentage. For example by 10 or 20%, or even doubling every line.
- Look for the lines that are binding for some time-steps in the original problem (we have seen that it generally corresponds to the first lines of the network) and expand them all by a certain percentage.

These propositions limit the number of scenarios to the number of increased percentage factors. However, if we had something like "choose to expand or not each line by a factor of 10%", the number of possibilities grows immediately to $2^{29}$ in our case (ignoring secondary lines). Putting decision variables on every line does not seem solvable in a realistic amount of time.

# Conclusion

In the introduction, we identified three main objectives for this thesis : test the tractability of the SOCP model on capacity expansion problems, identify the behavior of low-voltage networks in presence of high decentralized production and identify the incentives for storage investment and the impact on the behavior of the network. We will here briefly sum up the results we obtained that are related to theses objectives.

In the two first chapters, we showed that the SOCP model presented in [5] could be extended to become a multi-time-step capacity expansion problem while maintaining convexity properties. We also showed that for a fixed local price at substation node (TLMP), the dual variable of the power balance constraint at each distribution node could be interpreted as the local (or locational) marginal price of power at this node (DLMP). In theory, if prosumers were facing locational marginal prices, we could make the social optimum and the individual optimum coincide. This is true for the economic dispatch problem (how should everyone produce) as well as for the optimal capacity expansion problem.

In chapter 4, we exposed the results we obtained from running our model on a realistic test network. Analyzing our results led us to the following conclusions:

- The SOCP model is computationally tractable and make possible to solve capacity expansion problems on real-sized network. Our model was running in less than 100 seconds on a portable computer for a network of 29 households and an horizon of 672 time-steps.
- High decentralized production levels would lead to over-voltage problems in the network if voltage were not controlled.
- Control on voltage variation and desynchronization between times of high consumption and times of high production lead to a high curtailment percentage (around 30 % of the yearly production in our on-grid configuration, almost the totality in off-grid configuration).
- The curtailment, optimal battery investment and locational marginal prices can be significantly different in function of the position in the network. The direction of the prices variations (increasing or decreasing along the line) depends on the direction of flows in the network (situation of consumption or over-production).
- Although battery investment looks like a reasonable way to tackle the curtailment, current prices make heavy investment in batteries not profitable from a social optimum point of view. The optimal investment for our network is limited to a capacity of a few kWh but the optimal investment capacity grows fast with decreasing batteries prices. This solution should therefore not be completely overlooked in the future.
- Since optimal battery sizing only partially prevents the curtailment of decentralized generation, we should be very careful when heavily investing in decentralized generation such as PV panels. This suggest we could also use our SOCP model to do capacity extension on decentralized generation as proposed in the extensions.

Finally, in Chapter 5, we compared the incentives given by different models of retail pricing. We observed that for high decentralized generation, most models would result in production levels that would violate network voltage constraints. Those models could therefore not exist without external control on voltage, even if a model such as "prosumer pricing" already gives slightly better incentives to avoid over-voltages problem. However, at the moment there seems to exist no model differentiating prices as a function of the position in the network. Such a model would be a natural way to move closer to the social optimum, especially by favoring solar production close to the substation node and by penalizing solar production at end of lines.

# Bibliography


[1] Michael Caramanis, Elli Ntakou, William W Hogan, Aranya Chakrabortty, and Jens Schoene. Co-optimization of power and reserves in dynamic t&d power markets with nondispatchable renewable generation and distributed energy resources. *Proceedings of the IEEE*, 104(4):807–836, 2016.

[2] Gerald Thomas Heydt, Badrul H Chowdhury, Mariesa L Crow, Daniel Haughton, Brian D Kiefer, Fanjun Meng, and Bharadwaj R Sathyanarayana. Pricing and control in the next generation power distribution system. *IEEE Transactions on Smart Grid*, 3(2):907–914, 2012.

[3] Rabih A Jabr. Radial distribution load flow using conic programming. *IEEE transactions on power systems*, 21(3):1458–1459, 2006.

[4] Javad Lavaei and Steven H Low. Zero duality gap in optimal power flow problem. *IEEE Transactions on Power Systems*, 27(1):92–107, 2012.

[5] Masoud Farivar and Steven H Low. Branch flow model: Relaxations and convexification—part i. *IEEE Transactions on Power Systems*, 28(3):2554–2564, 2013.

[6] Qiuyu Peng and Steven H Low. Distributed algorithm for optimal power flow on a radial network. In *Decision and Control (CDC), 2014 IEEE 53rd Annual Conference on*, pages 167–172. IEEE, 2014.

[7] Steven H Low. Convex relaxation of optimal power flow—part i: Formulations and equivalence. *IEEE Transactions on Control of Network Systems*, 1(1):15–27, 2014.

[8] Steven H Low. Convex relaxation of optimal power flow—part ii: Exactness. *IEEE Transactions on Control of Network Systems*, 1(2):177–189, 2014.

[9] Burak Kocuk, Santanu S Dey, and X Andy Sun. Strong socp relaxations for the optimal power flow problem. *Operations Research*, 64(6):1177–1196, 2016.

[10] Philipp Fortenbacher, Martin Zellner, and Göran Andersson. Optimal sizing and placement of distributed storage in low voltage networks. In *Power Systems Computation Conference (PSCC), 2016*, pages 1–7. IEEE, 2016.

[11] Alexandre LATERRE and Emmanuel DE JAEGER. Distributed algorithm for optimal power flow on multiphase distribution networks.

[12] Anthony Papavasiliou. Analysis of distribution locational marginal prices. *IEEE Transactions on Smart Grid*, 2017.

[13] Niels Leemput. *Grid-supportive Charging Infrastructure for Plug-in Electric Vehicles*. PhD thesis, Polytechnic University of Catalonia, 2015.

[14] A Delnooz, D Six, C Mol, and E Gielen. State-of-the-art in business models for charging services: The evcity approach. In *European Electric Vehicle Conference (EEVC)*, pages 1–8, 2012.

[15] ME Baran and Felix F Wu. Optimal sizing of capacitors placed on a radial distribution system. *IEEE Transactions on power Delivery*, 4(1):735–743, 1989.

[16] Mesut E Baran and Felix F Wu. Optimal capacitor placement on radial distribution systems. *IEEE Transactions on power Delivery*, 4(1):725–734, 1989.

[17] Ahmed Elsheikh, Yahya Helmy, Yasmine Abouelseoud, and Ahmed Elsherif. Optimal capacitor placement and sizing in radial electric power systems. *Alexandria Engineering Journal*, 53(4):809–816, 2014.

[18] S Neelima and PS Subramanyam. Optimal capacitor placement in distribution networks using differential evolution incorporating dimension reducing power flow method. In *Innovative Smart Grid Technologies-India (ISGT India), 2011 IEEE PES*, pages 396–401. IEEE, 2011.

[19] Johannes Michael Grothoff. Battery storage for renewables: market status and technology outlook. Technical report, Technical Report January, International Renewable Energy Agency (IRENA), 2015.

[20] Anthony Papavasiliou. *Optimization Models in Electricity Markets*. Université Catholique de Louvain, 2016.

[21] Martin Zellner. Economic assessment of distributed and centralized storage in distribution networks. 2015.

[22] Lingwen Gan, Na Li, Ufuk Topcu, and Steven H Low. Exact convex relaxation of optimal power flow in tree networks. *arXiv preprint arXiv:1208.4076*, 2012.

[23] K Mani Chandy, Steven H Low, Ufuk Topcu, and Huan Xu. A simple optimal power flow model with energy storage. In *Decision and Control (CDC), 2010 49th IEEE Conference on*, pages 1051–1057. IEEE, 2010.

[24] Dennice Gayme and Ufuk Topcu. Optimal power flow with large-scale storage integration. *IEEE Transactions on Power Systems*, 28(2):709–717, 2013.

Rue Archimède, 1 bte L6.11.01, 1348 Louvain-la-Neuve **www.uclouvain.be/epl**